Dimensions of Marine Phytoplankton Diversity

Stephanie Dutkiewicz[1,2], Pedro Cermeno[3], Oliver Jahn[1], Michael J. Follows[1], Anna E. Hickman[4], Darcy A.A. Taniguchi[5], Ben A. Ward[4]

1. Department of Earth, Atmospheric and Planetary Sciences, Massachusetts Institute of Technology, Cambridge, MA, 02139, USA
2. Center for Climate Change Science, Massachusetts Institute of Technology, Cambridge, MA, 02139, USA
3. Institut de Ciencies del Mar, CSIC, 08003 Barcelona, Spain
4. Ocean and Earth Sciences, University of Southampton, National Oceanography Centre Southampton, Southampton, SO14 3ZH, United Kingdom.
5. Department of Biological Sciences, California State University San Marcos, San Marcos, CA,92096 USA

Correspondence to: Stephanie Dutkiewicz (stephd@mit.edu)

Abstract. Biodiversity of phytoplankton is important for ecosystem stability and marine biogeochemistry. However, the large-scale patterns of diversity are not well understood and are often poorly characterized in terms of statistical relationships with factors such as latitude, temperature, and productivity. Here we use ecological theory and a global trait-based ecosystem model to provide mechanistic understanding of patterns of phytoplankton diversity. Our study suggests that phytoplankton diversity across three dimensions of trait space (size, biogeochemical function, and thermal tolerance) is controlled by disparate combinations of drivers: the supply rate of the limiting resource, the imbalance in different resource supplies relative to competing phytoplankton demands, size-selective grazing, and transport by the moving ocean. Using sensitivity studies we show that each dimension of diversity is controlled by different drivers. Models including only one (or two) of the trait dimensions will have different patterns of diversity than one which incorporates another trait dimension. We use the results of our model exploration to infer the controls on the diversity patterns derived from field observations along meridional transects in the Atlantic and to explain why different taxa and size classes have differing patterns.

1 Introduction

Phytoplankton are an extremely diverse set of microorganisms spanning more than 7 orders of magnitude in cell volume (Beardall et al., 2008) and an enormous range of cell morphologies, bio(geo)chemical functions, elemental requirements and trophic strategies. This range of traits play a key role in regulating the biogeochemistry of the ocean (e.g. Cermeño et al., 2008; Fuhrman 2009) including the export of organic matter to the deep ocean (Falkowski et al. 1998; Guidi et al, 2009), which is critical in oceanic carbon sequestration and contributes to modulation of atmospheric CO_2 levels and climate. Biodiversity is also important for the stability of the ecosystem structure and function (e.g. McCann 2000; Ptacnik et al 2008; Cermeño et al. 2016), though the exact nature of this relationship is still debated. Studies suggest that diversity loss

appears to coincide with a reduction in primary production rates and nutrient utilization efficiency (Cardinale et al., 2011; Reich et al., 2012), thereby altering the functioning of ecosystems and the services they provide. Diversity is important, but what factors control diversity still remains an elusive problem.

35   Numerous studies have attempted to understand or predict observed patterns of biodiversity or species richness of marine phytoplankton by correlating with factors such as temperature and latitude (see e.g. Hillebrand and Azovsky, 2001; Hillebrand, 2004; Irigoien et al. 2004; Smith et al, 2007; Rodriguez-Ramos et al 2015; Powell and Glazier, 2017; Righetti et al. 2019). The metabolic theory of ecology posits that temperature could control the probability of mutation and speciation leading to more diversity at higher temperatures (see e.g. Allen et al 2007). However, a recent study suggests a unimodal statistical relationship

40   between diversity and temperature (Righetti et al., 2019). Studies have also proposed a latitudinal dependence of diversity (e.g. Chust et al 2012), though the shape of that dependence is unclear. Chaudary et al (2016) for instance suggests a bimodal distribution, and a study of the Cenozioc fossil records suggest that the diversity of diatoms may actually have increased towards the poles (Powell and Glazier, 2017). However, Rodriguez-Ramos et al (2015) found little evidence of a relationship between nano- and micro-phytoplankton species richness and either temperature or latitude after enforcing consistency of data

45   sets. Additionally, there is evidence suggesting that increased dispersal (up to a point) could increase diversity (Matthiessen and Hillebrand, 2006), and diversity was related to meso-scale features in a study in the North Atlantic (Mousing et al, 2016). There has been a debate as to how productivity links to diversity (see e.g. review by Smith, 2007). Again, by standardizing data sets to correct for differences in sampling efforts, only weak (or no) correlation between phytoplankton diversity and productivity emerges from basin-scale data sets (Cermeno et al 2013; Rodriguez-Ramos et al., 2015) suggesting that previously

50   reported connections might be skewed by sampling biases (Cermeno et al, 2013). However, it also appears that biotic factors can potentially impact diversity: The importance of top down control has been suggested by the experiments of Worm et al (2002). Multiple factors appear to be likely important, but correlations with multiple co-occurring environmental factors do not satisfactorily explain diversity patterns (e.g. Rodriquez-Ramos et al 2015). There remains no holistic understanding of phytoplankton diversity and its drivers.

55   Recent theoretical work (e.g. Vallina et al 2014b; 2017; Treseleer et al 2015) suggest that breaking diversity down into traits can be useful. Vallina et al (2017) also suggested that a variety of traits respond differently to environmental factors. The importance of multiple phytoplankton traits in setting community structure has previously been expounded (e.g. Litchman et al 2010, Acevedo-Trejos et al., 2015). Theory and models have considered several different phytoplankton traits and environmental drivers to explain diversity. In one study, different temperature dependencies and nutrient affinity trade-offs

60   allowed phytoplankton to have similar lowest subsistence nutrient requirements (as described in Tilman, 1977; 1982) that allowed sustained co-existence (Barton et al 2010). Other studies explored the importance of top-down control (Prowe et al, 2012; Vallina et al., 2014a, Ward et al 2014). A positive relationship between diversity and productivity was found when a model captured only different size classes, but no temperature differences (Ward et al., 2012; 2014). A series of studies also showed that mesoscale features and dispersal enhanced diversity (Levy et al. 2014; 2015; Clayton et al 2013), also revealing

65   that hot spots of diversity occurred in regions of high mixing (Clayton et al 2013).

In this study we will almost exclusively consider diversity in terms of "richness", the number of locally co-existing species. This definition is often referred to as alpha-diversity. We focus on richness here as the ecological theories we will use explain co-existence, rather than other common metrics of diversity such as Shannon Index or evenness. We also do not consider species present at extremely low population densities, the so-called rare biosphere.

70 In this study we seek to disentangle the multiple, sometimes conflicting, results from models and observational studies and seek to explain at least some of the controls on diversity. We employ ecological theories and a trait-based global model. We use observed patterns of diversity along meridional transects in the Atlantic as motivation and as illustration of the utility of this study. By using model and theory, we explore the mechanistic drivers of the modelled diversity. We conduct sensitivity experiments to test the intuition that the theoretical framework provides. However, on a cautionary side, this study tells us

75 about the diversity in the model world. Though our model is complex, it still missed many of the traits of the real ocean microbial communities.

This study synthesises much of the understanding that we have gained through previous modelling and theoretical studies (e.g. Dutkiewicz et al, 2009,2012, 2014; Ward et al 2013; 2014; Levy et al 2014). What is unique here is bringing these all together, addressing disparities in previous works and providing insight into the multiple interacting mechanisms that drive diversity.

80 We find that this can only be done by acknowledging that diversity along different axes of traits (e.g. size, biogeochemical function, thermal norms) each has their own set of drivers. And this is turn suggests that no single or combined set of environmental variables will be able to explain patterns of diversity in the ocean.

2. Methods

85 ### 2.1 Atlantic Meridional Transect (AMT) Observations

As an illustrative example from field observations, we used data of species composition, abundance and cell size in the range of nano- and micro-phytoplankton from samples collected in marine pelagic ecosystems. The data come from transects sampled during September to October 1995 (AMT-1), April to May 1996 (AMT-2), September to October 1996 (AMT-3), and April-May 1997 (AMT4). These cruises crossed the same regions of the Atlantic Ocean by a similar route. At each station,

90 2 replicate seawater samples were preserved, one with 1 % buffered formalin (to preserve calcite structures) and the other with 1 % final concentration Lugol's iodine solution. After sedimentation of a sub-sample for 24 h (Utermöhl's technique), cells were measured and counted with an inverted microscope at x187, x375 and x750 magnifications to cover the full ensemble of nano- and micro-phytoplankton, and identified to the lowest possible taxonomic level (usually species level). The volume of water samples used for sedimentation varied between 10 and 100 ml, according to the overall abundance of phytoplankton as

95 shown by the fluorometer. At least 100 cells of each of the more abundant species were enumerated. Here diversity is determined as richness, which here is defined as the number of species detected in sample volumes in the range 10-100 ml. Results from the coccolithophore and diatom species richness from this dataset have previously been shown in Cermeno et al

(2008). Cell volume was calculated by assigning different geometric shapes that were most similar to the real shape of each phytoplankton species. A mean cell volume was assigned for each phytoplankton species. Cells were separated into diatoms, coccolithophore and dinoflagellate groups. Here these data are used to determine total species richness (number of co-existing species) of all the nano- and micro-eukaryotes (Fig 1a), but also species richness within diatom, dinoflagellate and coccolithophore groups (Fig 1b), as well as number of species in three size classes (2-10 µm, 10-20 µm, >20 µm, Fig 1c). Given how these data are compared to model output (see below) we purposely neglect the rare biosphere, so do not attempt any techniques such as rarefaction to account for rare species.

2.2. Numerical Model

The model follows from Dutkiewicz et al (2015a) in terms of biogeochemistry, plankton interactions, and transmission of light as described by the tables and equations of that paper. However, the types of phytoplankton and zooplankton differ in that they include greater diversity. Here we briefly provide an overview of the model and detailed descriptions of the more complex ecosystem. More details of pertinent parameterizations and parameters can be found in the Supplemental Text S1, Supplemental Fig S1 and S2, and Supplemental Tables S1 and S2; the full set of equations and remainder of biogeochemical parameters can be found in Dutkiewicz et al (2015a).

The biogeochemical/ecosystem model resolves the cycling of carbon, phosphorus, nitrogen silica, iron, and oxygen through inorganic, living, dissolved and particulate organic phases. The biogeochemical and biological tracers are transported and mixed by the MIT general circulation model (MITgcm, Marshall *et al.*, 1997) constrained to be consistent with altimetric and hydrographic observations (the ECCO-GODAE state estimates, Wunsch and Heimbach, 2007). This three-dimensional configuration has coarse resolution (1°×1° horizontally) and 23 levels ranging from 10m in the surface to 500m at depth. At this horizontal resolution, the model does not capture mesoscale features such as eddies and sharp fronts, a limitation of the model that must be kept in mind when considering the results.

We use a complex marine ecosystem that incorporates 350 phytoplankton types that can be described in 3 "dimensions" of trait space (schematically shown in Fig 2): size, biogeochemical function, and temperature tolerance. Within the "size" dimension we include 16 size classes spaced uniformly in log space from 0.6 µm to 228 µm equivalent spherical diameter (ESD). Within the "biogeochemical function" dimension we resolve diatoms (that utilize silicic acid), coccolithophores (that calcify), mixotrophs (that photosynthesize and graze on other plankton), nitrogen fixing cyanobacteria (diazotrophs), and pico-phytoplankton. We resolve 4 size classes of pico-phytoplankton (from 0.6 to 2 µm ESD), 5 size classes of coccolithophores and diazotrophs (from 3 to 15 µm ESD), 11 size classes of diatoms (3 to 155 µm ESD), and 10 mixotrophic dinoflagellates (from 7 to 228 µm ESD). Additionally, we resolve a "temperature norm" trait axis, where phytoplankton growth rates are defined over a specific range of temperatures (Fig 3) by an empirically motivated function (e.g. Thomas et al, 2012, Boyd et al, 2013). We include 10 different norms. Thus for any size class within a functional group there are 10 different unique phytoplankton types (as demonstrated schematically in Fig 2) with different range of temperatures over which the cells will

grow. Warmer adapted types are assumed to grow faster as suggested empirically (Eppley, 1972, Bissenger et al, 2008) and from enzymatic kinetics (Kooijman, 2000). In total we resolve 350 phytoplankton "types" within 16 size classes, 5 biogeochemical functional groups, and 10 temperature norms.

Phytoplankton parameters influencing maximum growth rate, nutrient affinity, grazing, and sinking are parameterized as a power function of cell volume: aV^b (following Ward et al., 2012; see Supplemental text S1.2 and Table S2). Thus many size classes can be described by just two coefficients (*a,b*) per parameter. Maximum growth rate is parameterized (i.e. the *a,b* in the above equation) as distinct between functional groups (as suggested by observations in Fig 4a, see also Buitenhuis et al 2008; Sommer et al 2017). The smallest diatoms (3μm) have the highest maximum growth rates. Plankton smaller than 3μm have an increase of growth rate with size, and those larger than 3μm have a decrease of growth rate with size. This unimodal distribution has been observed (e.g. Raven 1994; Bec et al 2008; Finkel et al 2010; Maranon et al 2013; Sommer et al 2017) and explained as a trade-off between replenishing cell quotas versus synthesizing new biomass (Verdy et al., 2009; Ward et al 2017). There are also specific differences between functional groups in cell elemental stoichiometry and palatability to grazers (diatoms and coccolithophores, with their hard surface covering deter grazers, see e.g. Monteiro et al., 2016, Pančić et al., 2019). The smallest phytoplankton have the highest affinity for nutrients (Edwards et al., 2012) as a result of the lower surface to volume ratio found in larger cells (Kiorboe 1993, Raven, 1994).

The model includes spectral irradiances, and each functional group has different spectra for absorption (as a result of group specific accessory pigments) and scattering of light. The absorption spectra are flatter with larger sizes following Finkel et al (2000) to account for self-shading, and scattering spectra are also influenced by size following Stramski et al (2001) (see Supplemental text S1.3, Supplemental Fig S1). The simulation uses Monod kinetics, and C:N:P:Fe stoichiometry are constant over time (though differ between phytoplankton groups). Chl-a for each phytoplankton types varies in time and space depending on light, nutrient and temperature conditions following Geider et al (1998). Following empirical evidence, mixotrophic dinoflagellates are assumed to have lower maximum photosynthetic growth rates than other phytoplankton of the same size (Tang, 1995; Fig 4a).

We resolve 16 size classes of zooplankton (from ESD 6.6μm to 2425μm) that graze on plankton (phyto- or zoo-) 5 to 20 times smaller than themselves, but preferentially 10 times smaller (Hansen et al., 1997; Kiorboe 2008, Schartau et al 2010). Maximum grazing rate is a function of size (following Hanson et al. 1997), though the four smallest grazers are assumed to have the same maximum grazing rates (Supplemental Fig S2). Here the smallest grazers do not have a clear difference in grazing related to size (following the data compilation of Taniguchi et al, 2014). Mixotrophic dinoflagellates also graze on plankton with the same predator-prey ratios as the zooplankton, and have size-dependent maximum grazing rates. However, they have lower maximum grazing rates than zooplankton of the same size (Jeong et al., 2010, Supplemental Fig S2). We use a Holling III grazing function (Holling, 1959). Sensitivity studies with a Holling II parameterization show that the results here are not sensitive to this choice.

We perform a "default" simulation (EXP-0) for 10 years. The ecosystem quickly (within 2 years) reaches a quasi-steady state. Here we show results from the 5th year of the simulation, but note that the patterns of biogeochemical and ecologically relevant

165   output and diversity are not significantly different if we instead used the 10th year. We also conducted a series of sensitivity experiments, where we alter either physical or ecosystem assumptions to provide evidence for the controls of diversity (Table 1).

As mentioned in the introduction, in this study we primarily discuss diversity in term of "richness" defined here as the number phytoplankton types that co-exist at any location above a biomass threshold. We, in particular, look at the annual mean of the

170   instantaneous surface richness (though see Supplemental for examples with depth). Technically, we use a threshold value (10^{-5} mmolC/m^3) to determine whether a phytoplankton type is present or absent in a given community. This value would convert to about 10 *Prochlorococcus* cells/ml (typical oligotrophic waters are above 10^3 cells/ml), or only a tiny fraction (10^{-4}) of a larger diatom cell/ml. Thus, this definition neglects rare species, often at abundances in the order of individuals per liter, that would be difficult to separate from numerical noise. This is why we do not account for the rare species in the AMT observations

175   discussed above. The value of richness can be altered depending on the threshold chosen, but the patterns and results discussed below remain robust. We also emphasise that the level of richness that the model captures, though large for a model, is orders of magnitude lower than the real ocean. Thus, this is not a fully comprehensive study of diversity or species richness, but does never-the-less provide a promising avenue for understanding some of the controls on diversity.

3. Results

180   **3.1. Diversity Observations along the AMT**.

The four Atlantic Meridional Transect (AMT) cruises provide a large-scale consistent dataset of phytoplankton diversity including microscopic counts of diatoms, coccolithophores and dinoflagellates. Such microscopic measurements depict species richness patterns of abundant taxa but miss much of the rare biosphere. This dataset shows distinct large-scale patterns (Fig 1a), with high richness (as determined by number of co-existing species) on the northern edge of the Southern Ocean, in the

185   Canary upwelling, low richness in the subtropical gyres, and slightly elevated richness in the equatorial region.

However, the patterns of richness are very different if we look only within a single functional group (e.g. diatoms, Fig 1b) or within a specific size class (Fig 1c). Diatoms exhibit higher diversity in the Southern Ocean than the other functional groups, while the diversity of coccolithophores and dinoflagellates is much more uniform across the transects. Among size classes, the smallest size category (2-10μm) has the highest diversity, while there is lower and more regionally varying diversity in the

190   larger size categories, with some regions having none of the largest size class (>20μm). This suggests that the controlling mechanism(s) on, for instance, diatom diversity is different to those controlling coccolithophore diversity, which also differs to what determines the diversity within different size classes. Indeed, modelling and theoretical work (e.g. Vallina et al 2014b; 2017; Terseleer et al 2014) have suggested that breaking diversity down into traits can be insightful. Thus, a starting point of our study is to separate out different dimensions of diversity.

195

3.2. Numerical Model

Model development was guided by evaluating against a range of in situ and satellite-derived observations (see Supplemental text S2 and Supplemental Figures S3-S8). We refer the reader to the fuller evaluation in the Supplemental text, but provide a brief version here. The model captures the patterns of low and high Chl-a seen in the satellite estimate (Supplemental Fig S4),
200 though underestimates the Chl-a in the subtropical gyres and over-estimates in the high latitudes. However, we note that satellite-estimated Chl-a has large uncertainties (Moore et al, 2009) especially in the Southern Ocean (e.g. Johnson et al 2013). The coarse resolution of the model does not capture important physical processes near coastlines, and lack of sedimentary and terrestrial supplies of nutrients and organic matter lead to Chl-a being too low in these regions. The underestimation of Chl-a in the gyres is also seen when comparing the model to the observations of surface Chl-a along the AMT (Fig 5b, Supplemental
205 Fig S6b). The model does capture the drawdown of nutrients in the gyres and the large increase of nutrient concentrations in the Southern Ocean (Fig 5a, Supplemental Fig S6a). However, the model over-estimates the amount of silicic acid in this ocean (seen also in the global evaluation, Supplemental Fig S3), likely a reflection of Si:C of the model diatoms being too low in the region.

The model individual types have plausible ranges (4 representative species shown in Supplemental Fig S9) compared to
210 distributions determined from thermal niches (e.g. Thomas et al., 2012) and statistical techniques from sparse observations (e.g. Barton et al. 2016). The model captures biomass in almost all size classes (Fig 6, Supplemental Fig S10a), though the largest size classes are underestimated. Traits not included in the model (e.g. buoyancy regulation, chain formation, symbiosis) are possibly more important for maintaining these large size classes. The model has biomass in all temperature norms (Fig 6, Supplemental Fig S10c), though with lower biomass in the coldest and warmest adapted suggesting the model parameterization
215 covers an adequate range of norms. There are some interesting eliminations (which match observations) such as coldest adapted smallest pico-phytoplankton and diazotrophs, and large warmest-adapted diatoms. The phytoplankton are complemented by a range of size classes of zooplankton (Supplemental Fig S11).

We evaluate the model's ability to capture the size distribution of phytoplankton as derived from satellite products (Fig 7a, Supplemental Fig S4, S5). Here we capture the ubiquitous pico-phytoplankton and the limitation of the larger size classes to
220 the more productive regions. The model pico-phytoplankton size class Chl-a is potentially slightly too low and the nano size class too high. Though we note that if we set the pico/nano break at the model 5th size class (just under 3μm) instead at the 4th (2μm) size class, the relative values are much more in line with the satellite product. We suggest that the satellite product division might not be that exact. The micro-size class matches in location to the satellite product but is too low as discussed above.

225 We also compare the model functional group distribution to the compilation of observations (Fig 7b, MAREDAT, Buitenhuis et al 2013, and references therein). Though the observations are sparse, we do capture the ubiquitous nature of the pico-phytoplankton, the limited domain of the diazotrophs (including observed lack of diazotrophs in the South Pacific gyre), the pattern of enhance diatom biomass in high latitude, and low in subtropical gyres. We over-estimate the coccolithophore

biomass relative to MAREDAT in many regions, but note that the conversion from cells to biomass in that compilation was
230 estimated to have uncertainties as much as several 100% (O'Brien et al., 2013). The MAREDAT compilation did not include a category for dinoflagellates. We also compare the model biomass of diatoms, coccolithophores and dinoflagellates along the AMT, though note that the conversion from cell counts to biomass in the observations has significant uncertainties. The model captures the much lower biomass of diatoms in the subtropical gyres than the other two functional groups, and higher in the Southern Ocean. Coccolithophore biomass is too low in the Southern Ocean in the model, likely due to the modelled smallest
235 diatom being parameterized as too competitively advantaged, but compares better in the rest of the transect than MAREDAT comparison above suggested.

In this study we mostly consider richness, the number of co-existing types, as a metric of diversity. However, we do discuss Shannon Index (another commonly used metric of diversity) later in the text. We will refer to "total" richness, i.e. the number of co-existing phytoplankton types, out of the 350 initialized in the model, at any location (Fig 8a). Here we specifically look
240 at the annual mean richness in the surface layer which is a good indicator of the diversity within the mixed layer (Supplemental Fig S12). We find lowest richness in the subtropical gyres and highest associated with the western boundary currents.

The model is designed to allow for richness within specific functional groups and size classes. A unique feature about this study is a comparison to the richness found in the AMT data (Fig 1, Supplemental Fig S7, S8). The model captures the low and high patterns of the AMT observations, though underestimates the diversity in the subtropical gyres. In these regions it is
245 likely that traits axes (e.g. symbiosis, colony formation etc) not captured in the model provide additional means for phytoplankton to co-exist. Excitingly the model also captures the differences in the diversity within functional groups and in size classes. Diatoms have much larger diversity in the Southern Ocean than the other functional groups, while coccolithophores and mixotrophic dinoflagellates diversity is much more uniform across the transect. The model captures the much higher diversity within the smallest size category (2-10μm) and the lower and much more regionally varying diversity
250 in the larger size category, including the lack of diversity in the largest size class (>20μm) in the subtropical gyres.

It is instructive to also consider richness along each of the dimensions of trait space. The number of size classes (irrespective of functional group or thermal norm) that co-exist in any location will be referred to as size class diversity (Fig 8b). We find that in high latitudes and along the equator, many size classes are present, while in the subtropical gyres only few, small-sized
255 classes survive (Fig 7a, Supplemental Fig S10a). We find that there are different patterns of richness when looking along the two other axes of traits (Fig 8c,d; Supplemental Fig S10b,c). Richness of biogeochemical functional groups is highest in the mid-latitudes, strongly linked to the distributions of diazotrophs (Fig 7b, Supplemental Fig S10b). In contrast, the diversity within temperature norms is maximum in the western boundary currents, in particular the Gulf Stream and Kuroshio, and high in coastal upwelling regions (e.g. off Peru and Canary) and along the northern boundary of the Southern Ocean.
260 The total richness is a complex integral function (i.e. multiplicative) of the three different trait dimensions. At first glance total diversity (Fig 8a) may look most like the thermal norm diversity (Fig 8d), but this is mostly because our eyes are drawn to the hotspots. In reality, total diversity patterns are strongly impacted by all three dimensions of diversity as will be shown more

clearly by the sensitivity experiments discussed later. We find that some trait dimensions are more (or less) important in different regions. For instance, thermal norm richness leads to the total richness hotspots (Fig 8a) in the western boundary currents and coastal upwelling regions. While reduction in functional groups and thermal norms counteract the increase in size classes in the Southern Ocean, all three dimensions together lead to the lowest total richness captured in the middle of the subtropical gyres.

4. Understanding the Dimensions of Diversity: Model and Theoretical Framework

None of these three dimensions can, in isolation, explain the controls on the total richness. Nor can we a priori understand the total richness. By using ecological theories and a series of sensitivity experiment (Table 1), we can begin to understand the mechanisms setting the different dimensions of diversity individually. Here, we step through each of the dimensions.

The theoretical frameworks are presented in the Appendix and are informed from the seminal work of Tilman (1977, 1982) and Armstrong (1994). Resource competition theory (Tilman 1977, 1982) has been extensively used in theoretical and experimental studies (e.g. Sommer 1986; Grover, 1991a,b; Huisman et al, 1994; Schade et al 2005; Miller et al., 2005; Wilson et al., 2007; Agawin et al 2007; Snow et al 2015) as well as linking to numerical models (Dutkiewicz et al., 2009; 2102; 2014; Ward et al., 2013) to explain aspects of community structure. The theoretical underpinning of size-selected grazing (Armstrong 1994) have similarly been used in many studies (e.g. Lampert, 1997, Kiorboe, 1993; 2008; Schartau et al 2010; Ward et al., 2014; Acevedo-Trejos et al., 2015). The appendix and the insight we develop in the rest of this section are in some sense a synthesis of many prior studies. Here, these theories are specifically directed at understanding diversity patterns, something that to our knowledge has not been done before.

4.1 Size Class Diversity

We find that the richness of cell sizes increases with the supply rate of the limiting nutrient (Fig 9). Theoretical predictions and previous model studies suggest that this should be the case when the resource requirements of phytoplankton increase with increasing size (appendix, Armstrong, 1994; Ward et al, 2014; Follows et al 2018). In the nomenclature of resource supply theory (Tilman, 1977), R^* of a phytoplankton type is the minimum resource concentration required for it to survive at steady state. In the absence of grazing, $R^* = \frac{k_R M}{\mu_{max} - M}$ where K_R is the resource half saturation constant, μ_{max} is the maximum growth rate and M is a loss rate (see appendix). The phytoplankton with the lowest R* will draw the nutrients down to this concentration and exclude all others. In our model, the smallest pico-phytoplankon have the lowest R^* and larger phytoplankton have subsequent higher R^* (Fig 4b). In this formulation, the smallest phytoplankton should out-compete all others. However, when we take grazing by a zooplankton (Z) into account, $R^* = \frac{k_R g Z}{\mu_{max} - g Z}$ where g is a per biomass grazing rate. Thus, R^* increases with increased grazing. When the grazing pressure is sufficiently strong on the smallest type, the R^* of the next smallest phytoplankton is reached and the two phytoplankton can co-exist. The smallest size class phytoplankton

and its grazer have their biomass capped and any increase in biomass is now due to the next size class (Armstrong 1994). This process continues to more and more size classes as we go from regions of low to high nutrient supply rates (Fig 9).

295 We note that the model is significantly more complex than the simple theoretical framework, including multiple limiting nutrients, multiple variants of one of those resources (NH_4, NO_2 and NO_3) with differing affinities, additional loss terms (e.g. sinking) as well as more complicated grazing and food web (rather than food chain). However, this framework still helps us understand the patterns of size diversity in the model.

In the model, some regions have different limiting nutrients (e.g. iron versus dissolved inorganic nitrogen), so the patterns of
300 size diversity from the total community are more complicated than considering only one nutrient supply rate. But, this process is nicely shown by the number of size classes within the diatom group alone increasing cleanly with the supply of silicic acid (Fig 9d). The fact that each size class is capped by grazing leads the distributions of size classes to be relatively even, especially in the highest nutrient regimes (shown by the Shannon Index, Supplemental text S3, Supplemental Fig S13).

To explore the importance of size-specific top-down control on diversity suggested by this theoretical construct, we conduct a
305 sensitivity experiment (EXP-1, Table 1), where we allow only one grazer to prey on all phytoplankton. We also do not allow for mixotrophy. We find that only the smallest size class in each functional group survives (Fig 10b, Supplemental Fig S14): the 0.6μm pico-phytoplankton and the 3μm diazotrophs, coccolithophores and diatoms. The dinoflagellates do not survive without mixotrophy. The size diversity reduces to one in most regions (Fig 11). This experiment highlights that size diversity (Fig 8b) is controlled not only by the rate of supply of the limiting nutrients, but also by size specific grazing (Armstrong 1994,
310 Poulin and Franks, 2010, Ward et al 2012).

The thermal norm richness of EXP-1 is very similar to the original "default" experiment (Fig 8d), and thus richness of this dimension is not (at least greatly) controlled by size specific grazing. Functional groups richness decreases as the dinoflagellates are no longer viable without mixotrophy. All other functional groups survive (Fig 10b, Supplemental Fig S14) and there is coexistence at the functional level; however, the patterns are different to the default experiment. In EXP-1 there
315 are significant changes to the biogeochemistry, including the primary production (lower) and subsequent changes to nutrient supplies. It is these biogeochemical changes that alter the functional richness patterns (discussed more below). However, the total diversity reduces dramatically (Fig 11, top row). Patterns of hot spots are however still apparent, but the increases in diversity with higher nutrient supply is no longer apparent.

We have used steady state theory to explain the co-existence of size classes. We contend that when looking at annual average
320 richness this theory provides insight even in non-steady state regions such as the highly seasonal latitudes. However, we do acknowledge that the processes are more complex in these regions. For instance, during times of resource saturated conditions (e.g. beginning of the spring blooms), the smallest diatoms, which are the fastest growing phytoplankton, will dominate (Dutkiewicz et al., 2009, see appendix). However, as the grazer of the smallest diatom increases, the phytoplankton net growth rate (growth minuses losses) decreases until the next fastest growing phytoplankton (whose net growth rate is higher since it
325 is not yet under grazer controlled) is able to grow in (Fig 12). Such a progression of size classes of diatoms has been observed using Continuous Plankton Recorder (CPR) data (Barton et al. 2013) and modelled for a coastal system (Terseleer et al, 2014).

This process of succession continues until nutrients are drawn down, allowing the pico-phytoplankton and mixotrophs to dominate in this more steady-state lower nutrient environment (as suggested by Margalef's mandala, Margalef, 1978). Given that annually there is an optimum condition for each of those size classes, they do all co-exist though at seasonally varying abundances (i.e. they never go extinct locally).

4.2 Functional Group Diversity

The size class and functional group classifications are not completely orthogonal as the "pico-phytoplankton" group is entirely composed of the 4 smallest size classes. We therefore use a similar explanation as to why pico-phytoplankton can coexist with the other functional types in low seasonality regions: the low R^* of pico-phytoplankton allows them to survive ubiquitously and other functional groups can only coexist where (or when) grazing pressures on the pico-phytoplankton and resource supplies are high enough.

We find that for the rest of the functional groups, co-existence is strongly controlled by the differences in their resource requirements and the imbalances in the supply rates of multiple resources (resource supply ratio theory, Tilman 1982, see appendix). For instance, slow growing diazotrophs can only co-exist with faster growing phytoplankton groups when there is an excess supply of iron and phosphorus delivered relative to the non-diazotrophs N:P and N:Fe demands (Fig 13a,b,c; Dutkiewicz et al. 2012; 2014; Ward et al., 2013; Follows et al 2018). In such locations, the non-diazotrophs are nitrogen limited, while the diazotrophs can fix their own nitrogen, and the excess P and Fe not utilized by the non-diazotrophs is available (appendix; Fig 13b,c).

Similar arguments explain where non-diatoms can co-exist with the fast-growing diatoms (Fig 13d). In regions where there is excess supply of dissolved inorganic nitrogen, phosphate, and iron relative to the diatom Si:N, Si:Fe, Si:P demands there can be co-existence (Fig 13e,f,g). In these locations (or occasions), diatoms are limited by silicic acid, and any excess N, P and Fe can be used by the other phytoplankton. When the excess supply is significantly high, non-diatoms can dominate. The high silicic acid supply in the Southern Ocean leads to lower diversity as the diatoms win out in all but the low nutrient summer months, when (in this simulation) pico-phytoplankton are the only other functional group to survive. In other seasonal regions, such as the northern North Atlantic (Fig 12), diatoms dominate at the beginning of spring, but coccolithophores can outcompete later in the summer when the diatoms become limited by availability of silicic acid.

The mixotrophs have two sources of resources: inorganic nutrients and other plankton. They are parameterized to photosynthesize slower than other phytoplankton (of the same size, as suggested by observations, Tang 1994; Fig 4a) and graze slower than other grazers (of the same size, Jeong et al., 2010; Supplemental Fig S2). They are advantaged over specialist autotrophs and heterotrophs when competition for both inorganic nutrients and prey is strong and, by using both, their R^* for each resource is lowered.

To demonstrate that differential nutrient requirements lead to much of the functional group co-existence, we conduct another sensitivity experiment (EXP-2, Table 1) where we force all functional groups to have the same resource requirements (e.g.

360   diatoms do not require silicic acid, diazotrophs cannot fix nitrogen, dinoflagellates cannot graze on other phytoplankton) and
       C:N:P:Fe ratios are the same for all types. All other growth and grazing parameterizations remain the same as in the default
       experiment. In EXP-2, the functional richness reduces dramatically (Fig 11), only pico-phytoplankton and diatoms survive
       (Fig 10c, Supplemental Fig S15). The diatoms are the ultimate opportunists (r-strategists) in this model, with the highest
       growth rate (Fig 4a), and survive when nutrient supplies are high enough. Without any differentiating nutrient requirements
365   relative to the other functional groups, they outcompete them. Pico-phytoplankton (the gleaners, k-strategists) survive in
       regions of lowest nutrient supply where their low R* and low grazing allows them to exclude the diatoms. Size class and
       thermal norm diversity change very little (Fig 11). Total diversity is reduced everywhere, but mostly in the lower latitudes
       where the loss of diazotrophs and coccolithophores has a high impact.

370   **4.3. Thermal Norm Diversity**

       We find that thermal norm richness is highest in the regions of the western boundary currents and other regions generally
       anticipated to have high levels of mixing of different water masses. Clayton et al (2013) identified a link between hot spots of
       diversity and eddy kinetic energy and the variance in sea surface temperature. Anticipating the role of currents and mixing of
       water mass (Clayton et al 2013, Levy et al 2014), in a third sensitivity experiment (EXP-3, Table 1) we do not allow transport
375   of plankton between grid cells, though we do allow diffusion vertically in the water column. Thus, this simulation is a collection
       of one-dimensional models with regard the plankton. However, nutrients and dissolved and detrital organic matter are allowed
       to be transported as in the default experiment. Thermal norm diversity decreases (Fig 11), and there are no longer hot spots.
       These results echo findings from Levy et al (2014), and clearly show the importance of mixing of water masses for maintaining
       thermal norm diversity. When temperature is fluctuating all phytoplankton with different temperature norms can survive
380   together provided their respective temperature optimal occur for long enough (Kremer and Klausmeier, 2017) or there is a
       constant supply of the types from upstream (Clayton et al., 2013). This is different from resources or grazing control where
       competition for limited resources is the main process controlling co-existence (or lack thereof), and as such we find greatest
       effect in EXP-3 on thermal norm diversity. Total diversity is reduced everywhere, but most dramatically in these hotspot
       regions. Both Clayton et al (2013) and Levy et al (2014) showed the importance of eddies in enhancing this process of transport
385   mediated diversity. Thus the hotspots in the default experiment would likely be even higher in a model that did resolve the
       mesoscale.
       We find in EXP-3 that the geographical size of almost all habitats (Fig 14, Supplemental Fig S16) is reduced. In the case of
       thermal norms, lack of transport allows for very little co-existence. For functional diversity, the pattern changes, but the
       maximum richness remains the same. This suggests that the boundaries of functional groups domains are expanded by transport
390   (see for instance the decrease expanse of diatoms in the gyres, Supplemental Fig S16 versus S10), but transport per se is not
       the ultimate controller. Domains for each size class also decrease (Fig 14, Supplemental Fig S16), but most dramatically for
       the larger size classes, and the two largest go extinct in this experiment. This suggests that transport also plays a role in

maintaining the grazer/phytoplankton links and that for classes with smaller domains and/or very low biomass this becomes more crucial. A few types have an increase in range, or in fact exist in EXP-3 and not in the original experiment (Fig 10d, 14,
395   Supplemental Fig S16). These are almost all the warmest adapted types that in EXP-3 have very small biomass and ranges. Thus, transport can also reduce domains of types with very small potential niches as the constant influx of less fit types from cooler regions is sufficient to overcome any competitive advantage of the locally superior warm-adapted types (see appendix).

5. Links to Diversity along the Atlantic Meridional Transect

400   Using the results of this study, we can hypothesize as to why richness of co-existing nano and micro eukaryotes along the AMT (Fig 1a, 15a) have the observed patterns. We consider the modelled diversity within the three dimensions along the transect (Fig 15b,c,d). All three dimensions have high diversity along the north edge of the Southern Ocean (labelled A in Fig 15), suggesting that all controls (supply rate of limiting nutrient, imbalance in supply of different nutrients, top-down control, and transport) are at play in setting the maximum richness seen here in both model and observations (Fig 1a,d). Thermal and
405   functional richness decrease southward, leading to the drop in total richness observed poleward. Absolute nutrient supplies are still high enough to maintain size diversity, but the N:Si supply ratios are no longer conducive to maintaining coccolithophores (Fig 13e,f,g) and their diversity decreases as is observed (Fig 1b,e). In this southernmost region there is also no longer the mixing of different water masses between subtropical and Southern Ocean to promote large thermal norm diversity. However, diatom diversity (due here to size classes) increases (Fig 1b,e), driven by the large gradient in silicic acid supply rate (Fig 9d).

410

All three dimensions have an even sharper decrease equatorward of the Southern Ocean boundary, leading to much lower total diversity observed into the South Atlantic subtropical gyre (labelled B in Fig 15). Here the lower absolute nutrient supply likely leads to reduction in size classes, silicic acid supply rates drop dramatically (Fig 9d) and functional diversity decreases. The lack of mixing of water masses reduces the thermal norm diversity. Nearer the equator (labelled C), both size and
415   functional diversity are high, leading to the observed increase in total diversity. Here an increased supply of nutrients (Fig 9) from equatorial upwelling, including slightly higher Si supply rates are probably important for allowing additional size classes and diatoms to exist. In the region of the Canary upwelling region (labelled D), there is an increase in diversity in the model and observations. Here increased size class and thermal norm diversity are possibly responsible, a result of the nutrient-rich upwelled water mixing with surrounding water masses as it is transported offshore (see Clayton et al 2014). The model
420   underestimates this increase since the model's coarse resolution does not capture the meso-scale filaments associated with these upwelling features found in the real ocean.

6. Limitations of this Study

This study must be understood within the context of the limitations of the model. Models are by definition simplified constructs
425   that attempt to capture the essence of a real system. The model here has a more complex ecosystem than many other marine models but is still limited in terms of the parameterization choices. For instance, the size dependent grazing assumes a 10 to 1 preference as suggested by observations and used in many other studies (Fenchel 1987; Kiorboe 2008, Ward et al., 2012, Baird et al., 2004). However, there are many examples of grazing that breaks these preference rules (Jeong et al 2010; Weisse et al 2016; Sommer et al, 2018). The model assumes fixed elemental ratios in the plankton. This too is an oversimplification, and
430   variable ability to store nutrients and modify cellular quotas is an important trait that likely allows for levels of co-existence (Edwards et al 2011). This level of stoichiometric complexity is not incorporated here. However, the model carries almost 750 unique tracers to account for all the phytoplankton, variable Chl-a, as well as the inorganic and organic pools. To include variable stoichiometry would add over 2000 more tracers that is computationally unfeasible for this study. Each functional group has a different absorption spectrum, though these are modified with size (see Supplemental text S1.3 and Supplemental
435   Fig S1); we recognise that this has a large implication for the pico-phytoplankton whose accessory pigments are quite different. Using a version of this model, but with differing absorption spectra for the pico-phytoplankton, Hickman et al (2010) showed that such difference was responsible for some niche separation, especially vertically. The results of this study should be interpreted in light of these and other simplifications.

The model considers only three axes of phytoplankton traits. We anticipate that additional axes such as morphology (e.g.
440   shape, spines), motility (e.g. flagella), chains and colony formation, nutrient storage abilities, and symbiosis will each have their own controlling mechanisms. Such traits might allow the model to capture more species, and particularly, more large-sized phytoplankton types. Previous studies have suggested other controllers of phytoplankton distributions when considering other traits, for instance the importance of trade-offs between nutrient acquisition and storage (e.g. Edwards et al 2011) or the effect of symbioses (e.g. Follett et al 2018; Treguer et al 2018). Here, we have specifically designed the model to only consider
445   the three dimensions for simplicity. Including additional trait dimensions will likely lead to alterations to the patterns of diversity, and will be important for follow on studies, especially as our knowledge of the trade-offs of each trait dimension becomes clearer. For instance, the fact that the model underestimates diversity in the subtropical gyres suggests that additional dimensions are likely important in these regions.

Our results are also dependent on the resolution of different axes of trait space. Likely in the real ocean there is a similar
450   (though more complex) coarse resolution of functional groups, but much higher (potentially continuous) resolution of size classes and thermal norms. Total diversity may therefore be influenced more by these two axes than established in this study. Our model only captures a tiny (probably orders of magnitude less) amount of the diversity found in the real ocean. Including more resolution along these axes and including additional trait axes would allow for further diversity but is beyond the scope of our study. This study should be viewed as only a step in the understanding controls of diversity and provide new evidence

455   to explain the 'paradox of the plankton' (Hutchinson, 1961). However, that we can capture the major patterns of the AMT (Fig 1, Supplemental Fig S7) suggest that we have included some of the most important mechanisms.

Given computational constraints with this complexity of ecosystem model, we have used a coarse resolution physical model that does not capture explicit meso- (or sub-) scale features. Previous studies (e.g. Clayton et al 2013; Levy et al 2014) have shown the importance of such features in modulating diversity. Meso- and sub-mesoscale features give rise to temporal

460   increases in nutrient supplies (see e.g. Clayton et al., 2017), and, according to our results, this suggests temporal increases in size classes during such events. Sub- and meso-scale mixing in frontal regions will also enhance species richness in hotspots (Clayton et al 2013), but also a general increase of species richness (Levy et al 2014).

7. Discussion

465   We have used ecological theories and a numerical model to examine the controls on phytoplankton diversity along a number of trait dimensions. We find that each dimension has a different set of controls. Observed "total" diversity is an integrated function of the richness along each trait dimension and is thus controlled by many different mechanisms. By focusing on the mechanisms, we can understand the patterns of diversity at the fundamental level. Such insight provides us with a perspective to predict changes that might occur in diversity in, for instance, a warming world.

470   Our results suggest that observed patterns of "total" diversity (or for any grouping of phytoplankton types, such as for nano and micro-eukaryotes along the AMT) are a result of multiple controllers: supply rate of limiting resource, imbalance in supply of different resources relative to competitors' demands, top-down control, particularly in terms of size-dependent grazing, and transport processes. The importance of both resource supply and resource imbalance (or resource supply ratio) has previously been demonstrated by Cardinale et al (2009) for lake habitats and more recently for other natural phytoplankton assemblages

475   (Lewandowska et al., 2016).

In this study we have synthesised previously known theory and a numerical model. The results explain why previous model results have had sometime contradictory results. In ecosystem models that only considered two dimensions of diversity (functional groups and thermal norms, Barton et al, 2010, Clayton et al 2014) different patterns where obtained relative to a model that only considered size (Ward et al., 2014). For instance, the hotspots of diversity in western boundary currents were

480   not apparent in the study of Ward et al (2014) since thermal norm diversity was not included in that study. Similarly, the lack of high diversity along the edge of the Southern Ocean in Barton et al (2010), seen in this study and in the AMT observations (Fig 1), was due to the lack of size trait dimension in that study. This stresses that "diversity" in models needs to be understood in terms of the traits that are included. This obviously bring up the questions raised in Section 6: What additional patterns will be apparent in models that include additional, or other, trait dimensions. An exciting avenue for future study.

485   The drivers we found in this study (supply rate of limiting resource, imbalance in supply of different resources relative to the better competitor's demands, size-dependent grazing, and transport processes) have little to do with factors such as temperature

or latitude that have been investigated by correlations to diversity patterns (see e.g. Hillebrand and Azovsky, 2001; Hillebrand, 2004; Irigoien et al. 2004; Smith et al, 2007; Rodriguez-Ramos et al 2015; Powell and Glazier, 2017). However, there may be some occasions when there are correlations between such factors as temperature and, for instance, nutrient supply rates, thereby somewhat confounding correlation and causation. Though observational studies have hypothesized a multi-factorial control on diversity in the ocean (e.g. Rodriquez-Ramos et al 2015), they were unable to find significant correlations with any combination of factors such as latitude, temperature or biomass, or even nutrient concentrations. Correlating with factors such as temperature, latitude is a logical first step for trying to understand observed patterns of diversity, as these are often the only additional data that is available from a field study, and for instance "latitude" could potentially stand in for a range of biotic and abiotic processes. Our study, however, suggests that, to some degree, these factors are unlikely to help disentangle controllers of diversity. For instance, in our study, it is the mixing of different temperature water masses, potentially hinted at by local temperature variances, rather than temperature itself, that is important at least for one dimension of diversity. A previous study focusing on the interactions between microbes (and hence community structure) showed little statistical links to nutrient concentrations (Lima-Mendez et al., 2015). However nutrient supply rates (a harder variable to measure) has been shown to strongly influence the taxonomic and size structure of marine phytoplankton communities (see e.g. Mouriño-Carballido et al. 2016). Diversity controls inferred by correlations with environmental factors or from niche modelling (e.g. Righetti et al 2019, who make use of statistical inferences on species biogeography), likely miss important drivers. For instance, biotic interactions (competition and grazing) and impacts of transport (two mechanisms we have shown to be important) cannot easily be captured using such statistical techniques.

Biomass and productivity are dictated by the supply rate of the limiting nutrient, and therefore our study found an increase in size diversity with increased productivity and biomass. This compares well to the observations of Marañón et al (2015) and Acevedo-Trejos et al (2018) who found an increase in size classes with higher productivity. However, we caution that it is nutrient supply rate (not productivity) that is the controlling mechanism. Obviously, nutrient supply rate (a bottom up process) cannot alone lead to high size diversity. Top down processes are essential for the build-up of size classes with higher nutrient supply (see also Poulin and Franks, 2010). Considering only correlations with productivity would lead one to miss this important biotic interaction as a control on diversity. In our model top-down control was size-specific grazing, but similar patterns could be achieved with kill-the-winner type parameterizations (Vallina et al 2014a) or imposing species-specific grazers or viruses.

Though transport of phytoplankton most strongly controls the thermal norm diversity, we did find that it modulates the extent of the regions for all traits. For instance, diatoms die out in the central subtropical gyres when transport is turned off in EXP-3, and the largest size classes become less competitive without transport (Fig 10d, Supplemental Fig S16). Our explanations of the different controls on the diversity along different trait axes should be understood as focusing on the most important components. The real system has multiple controlling mechanisms working together.

The discussion of marine phytoplankton diversity must also be considered in light of the limited, but also different types, of observational datasets (see review, Johnson and Martiny, 2014). Different techniques tend to capture just some aspects of

diversity, for instance different axes are distinguished when instruments measure just size (e.g. by Flow Cytometer, LIIST), pigments (e.g. though HPLC), or morphologic and taxon differences (e.g. microscopy). Only recently have studies incorporated diversity from a genomic perspective (e.g. de Vargas et al, 2015). Genomic diversity tends to capture a much higher diversity than other methods, with a long tail of rare species not captured by other measurement (Busseni, 2018). Thus "diversity" depends on the definition, and/or on the measurement used. Observational datasets are, however, sparse and only capture a small temporal and spatial pattern of biodiversity. The key to having consistent datasets (e.g. Rodriguez-Ramos et al, 2015; Sal et al 2013), or that sampling biases might skew results (Cermeno et al 2013) have only recently become commonly understood.

8. Conclusions

In this study we have disentangled some of the multiple controls on marine phytoplankton species richness (or types), a metric of diversity. We have shown through theory and a model that diversity within different dimensions of phytoplankton traits are controlled by disparate drivers. The number of co-existing size classes of phytoplankton is largely controlled by the magnitude of the limiting resource supply rate and the strength of the size-specific top-down processes; functional groups co-existence is partly controlled by the imbalance in the supply rate of different resources relative to competing species' demands; the number of phytoplankton types with different thermal optima that can co-exist is strongly controlled by the amount of mixing of different water masses. Transport in general expands the range of phytoplankton habitats and leads to higher local diversity. That each controller affects a different dimension of diversity is important to explain why diversity patterns in models that include only one or two of the traits will have different results to one that includes all three. Likely including other traits (e.g. morphology, symbioses) controlled by different (as yet not understood) mechanisms will lead to additional components to the patterns of diversity.

This study offers an explanation to why there have often been conflicting results in observational studies that have attempted to link diversity to factors such as temperature or productivity. Even when they do show correlations with diversity, it can sometimes be only because such factors are also correlated with some of the actual drivers (such as nutrient supply rates), and results will also be specific to the dimensions of diversity measured. Models such as this one, though still only capturing a tiny amount of the full diversity of the ocean, can be a good tool to address both consistency and sampling biases, as well as providing insight into controlling mechanisms as we have done here. By understanding the mechanistic controls on diversity we are in a better position to understand how diversity might have been different in the past, how it changes with interannual variability, and how it might alter in a future ocean.

Code availability: The global physical/circulation model (MITgcm) is available at http://mitgcm.org and the ecosystem component is available from git://gud.mit.edu/gud1. Version and modifications used for this study are available at https://doi.org/10.7910/DVN/EOTT9H

Data availability: Model output used in this study is available at https://doi.org/10.7910/DVN/JUQCFG

555

Appendix

In this appendix we detail the theoretical framework we mention in the main text. This framework starts from the simplest system of equations to define the marine ecosystem. We note that the computer model discussed in the main text has much more complex equations, including temperature and light constraints on growth, multiple limiting nutrients, multiple variants

560   of one of those resources (NH_4, NO_2 and NO_3) with differing affinities, additional loss terms (e.g. sinking) as well as more complicated parameterization of grazing and a food web including carnivorous zooplankton.

Theory: We consider a system of phytoplankton biomass (B) sustained by nutrients (R):

$$\frac{dR}{dt} = -\mu_{max}\frac{R}{R+k_R}B + S_R \qquad\qquad\qquad\qquad \textit{Eq 1}$$

565    $$\frac{dB}{dt} = \mu_{max}\frac{R}{R+k_R}B - MB \qquad\qquad\qquad\qquad \textit{Eq 2}$$

where μ_{max} is maximum growth rate, k_R is half saturation constant for growth, S_R is supply of resource R and M is the phytoplankton loss term (we will consider different assumptions of M below).

A1. Steady State: Here we synthesise the theoretical underpinning that we have previously presented (Dutkiewicz et al., 2009;

570   Ward et al., 2013; Ward et al., 2014; Levy et al 2014; Follows et al. 2018). Those studies have in turn been informed from the seminal work of Tilman (1982) and Armstrong (1994).

We assume steady-state and solve the biomass equation (Eq 2):

$$R^* = \frac{k_R M}{\mu_{max}-M} \qquad\qquad\qquad\qquad \textit{Eq 3}$$

This is the concentration that the phytoplankton will draw the resource down to in steady-state. In a system with J

575   phytoplankton, the one with the lowest R_j^* will draw the nutrients down to this concentration and all others will be excluded.

A1.1. Grazing allows co-existence: If we now consider a system of J phytoplankton (B_j) and K zooplankton (Z_k), where each phytoplankton has a specific grazer, we can write the loss rate now as $M=m+g_{kj}Z_k$. Here g_{kj} is the per biomass grazing rate of zooplankton k on phytoplankton j, and m is a linear loss rate (resolving cell death and other losses). In this case:

580     $R_j^* = \frac{k_{Rj}\,(m+g_{kj}Z_k)}{\mu_{maxj}-(m+g_{kj}Z_k)}$ *Eq 4*

Note that this is not an explicit solution as Z_k is itself a complex function of the parameters. However, this equation can provide us with insight: with higher grazing R_j^* increases.

For a situation where R_j^* increases with size (in the absence of grazing), the smallest phytoplankton ($j=1$) will outcompete others in the absence of grazing. However as grazing pressure increases, $R_{j=1j=2}^*$ of this smallest type will increase. When this

585   $R_{j=1}^*$ becomes large enough it reaches the $R_{j=2}^*$ of the second smallest phytoplankton (assume for now that this plankton is not grazed) and the two phytoplankton will be able to co-exist. This situation occurs when there is higher resource supply (S_R) allowing for a larger biomass of both phytoplankton and zooplankton. With even higher nutrient supply, similar grazing control of the $j=2$ phytoplankton ($R_{j=2}^*$) will allow a third phytoplankton/zooplankton pair to co-exist with the others in the system. This system however does require a separate grazer per phytoplankton, or a strong kill-the-winner parameterization. This

590   theory explains the co-existence of several size classes in the ecosystem model (Fig 8b, Supplemental Fig S10). For more details, see Ward et al (2014) and Follows et al (2018).

A1.2. Multiple limiting resources allow co-existence: If we now consider a system of 2 phytoplankton (B_j, where j is 1 or 2) limited by different resources (R_i where i is *A or C*), we suggest that this system can allow for co-existence. To explore when

595   the two types can co-exist we expand Eqs 1 and 2 (where the biomass is in units of element *A)* such that:

$\frac{dR_A}{dt} = -\mu_{max1}\frac{R_A}{R_A+k_{RA1}}B_1 - \mu_{max2}\frac{R_C}{R_C+k_{Rc2}}B_2 + S_{RA}$ *Eq 5*

$\frac{dR_C}{dt} = -\mu_{max1}\frac{R_A}{R_A+k_{RA1}}\Upsilon_{AC1}B_1 - \mu_{max2}\frac{R_C}{R_C+k_{RC2}}\Upsilon_{AC2}B_2 + S_{RC}$ *Eq 6*

$\frac{dB_1}{dt} = \mu_{max1}\frac{R_A}{R_A+k_{RA1}}B_1 - M_1 B_1$ *Eq 7*

$\frac{dB_2}{dt} = \mu_{max2}\frac{R_C}{R_C+k_{RC2}}B_2 - M_2 B_2$ *Eq 8*

600   Where (Υ_{AC1}) is stoichiometric ratio requirements of B_1 for element *A* and *C*. S_{RA} and S_{RC} are the supply rate of nutrient A and C respectively. If one of the phytoplankton (B_1) has a much higher growth rate than the other (B_2) it will be a better competitor for both resources (*A* and *C).* We find, solving the above equations in steady state that co-existence is possible if:

$\frac{S_{RA}}{S_{RC}} > \Upsilon_{AC1}$ *Eq 9*

There must be excess supply of the resource limiting the slower growing phytoplankton relative the stoichiometric demands

605   of the faster growing phytoplankton for co-existence to occur.

For the case of a Fe limited diazotroph (which can fix their own nitrogen) and a faster growing DIN limited non-diazotroph, co-existence occurs when $\frac{S_{Fe}}{S_N} > \Upsilon_{NFe1}$, where Υ_{NFe1} is the stoichiometric demands of the non-diazotroph. We can write a similar in-equality for any other nutrient limiting the diazotrophs (e.g. P) and find that diazotrophs survive where both S_{Fe} and S_P are supplied in excess of the non-diazotroph requirements (Fig 13b,c). See Ward et al (2013) and Follows et al (2018) for

610   more details.

Similarly, the equations in steady state suggest that for slower growing non-diatoms to co-exist with the fast growing diatoms, the diatoms must be silicic acid limited. In a situation where the non-diatoms are DIN limited, then co-existence occurs if $\frac{S_N}{S_{Si}} > \Upsilon_{SiN1}$ where Υ_{SiNI} is the stoichiometric demands of the diatom. Again, similar in-equalities are applicable if other nutrients limit the non-diatoms (e.g. P, Fe) and we find that non-diatoms can exist where DIN, Fe and P are supplied in excess of the diatoms requirements (Fig 13e,f,g).

A1.3. Physical Transport can allow co-existence: As discussed in Levy et al (2014), physical transport can also modify R^*. Here were recognize that Eq 2 should be expanded for a moving ocean to:

$$\frac{dB}{dt} = \mu_{max}\frac{R}{R+k_R}B - MB + TB + VB \qquad \text{Eq 10}$$

Where T represents the per unit biomass advection of plankton, $T = -\frac{1}{B}\nabla.\vec{u}B$, where $\vec{u}$ is the local three dimensional velocity vector, and V represents per unit biomass vertical mixing, $V = \frac{1}{B}\frac{\partial}{\partial z}(K\frac{\partial B}{\partial z})$, where K is the vertical mixing coefficient and z indicates the vertical dimension. With these additions,

$$R^* = \frac{k_R(M-T-V)}{\mu_{max}-(M-T-V)} \qquad \text{Eq 11}$$

Thus T and V provide additional means for phytoplankton to have similar R^*. If a phytoplankton type is less competitive at a location, it can still have a similar R^* to a locally better adapted type if there is a steady influx of it from an upstream location. We clearly see this effect in the (generally) expanded biogeography of phytoplankton with advection relative to the experiment without advection (Fig 14, Supplemental Fig 16).

A2. Non-steady state: In a previous study (Dutkiewicz et al., 2009) we found that this steady state theory was applicable in a model in the subtropics and in the summer months in some of the high latitude regions. We contend that when looking at annual co-existence this theoretical understanding still provides insight even in non-steady state regions such as the highly seasonal high latitudes (as was done in Ward et al 2014). However, we do acknowledge that the processes are more complex in these regions. Such regions generally have a succession of dominance of different types. As long as there is a long enough period of favourable conditions for each type, the phytoplankton can co-exist, though with seasonally varying biomass. We explain the succession by considering Eq. 2 in a non-steady state:

$$\frac{1}{B}\frac{dB}{dt} = \mu_{max}\frac{R}{R+k_R} - M \qquad \text{Eq 12}$$

Such that the biomass normalized tendency term is dictated by the net growth rate: $(\mu_{max}\frac{R}{R+k_R} - M)$. At any moment (or with a short lag) the phytoplankton with the largest net growth rate can dominate (temporally).

A2.1. Spring Bloom: As suggested in Dutkiewicz et al (2009), the fastest growing phytoplankton will dominate at the beginning of the spring bloom when the nutrients are plentiful $\frac{R}{R+k_R}\sim 1$, and grazing is small, such that Eq 12 reduces to:

$$\frac{1}{B}\frac{dB}{dt} = \mu_{max} \qquad\qquad Eq\ 13$$

That is the phytoplankton with the largest μ_{max} will dominate. In the model here, this is the smallest diatoms.

645 **A2.2. Grazing allows co-existence:** If we now consider two phytoplankton (B_1, B_2) both limited by the same nutrient, R, and each having its own specific grazer (Z_1, Z_2), so that $M=m+g_{kj}Z_k$. If we assume $\mu_{max1} > \mu_{max2}$, then B_1 will dominate when there is no grazer control. However, when Z_1 is large enough, and Z_2 is small or negligible, it is possible for

$$\mu_{max1}\frac{R}{R+k_{R_1}} - m - g_{11}Z_1 < \mu_{max2}\frac{R}{R+k_{R_2}} - m \qquad\qquad Eq\ 14$$

In this case B_2 can grow in and potentially dominate the system temporarily. Similarly, as grazing control limits B_2, a third
650 species with slower growth but also lower grazing might be able to follow on the succession. This is shown in the model for a location in the North Atlantic with a succession of diatoms of increasing size in the spring bloom period (see Fig 12).

A2.3. Multiple limiting resources allow co-existence: We can also consider equations 7 and 8 (two phytoplankton types limited by different nutrient) in a non-steady state case. If B_1 is the faster growing species, it may still be outcompeted (at least
655 temporarily) by the slower growing species if

$$\mu_{max1}\frac{R_A}{R_A+k_{RA1}} < \mu_{max2}\frac{R_C}{R_C+k_{RC2}} \qquad\qquad Eq\ 15$$

That is, B_2 can succeed B_1 if the nutrient limitation of B_1 becomes severe enough that its net growth drops lower than its competitor which is limited (less) by a different nutrient. An example is a strongly silicic acid limited diatom later in the seasonal progression succeeded by a nitrate limited coccolithophores, as in the model example (Fig 12). Provided each type
660 has sufficiently long in favourable conditions each year, it will continue to co-exist at any location though at lower abundances for part of the year.

A2.4. Physical transport allows co-existence: We can use the biomass normalized tendency formulation to consider the circumstances were physical transport has an impact (see Eq 10):

665 $$\frac{1}{B}\frac{dB}{dt} = \mu_{max}\frac{R}{R+k_R} - M + T + V \qquad\qquad Eq\ 16$$

Temporarily a phytoplankton type might have the fastest tendency if T or V are particularly strong (i.e. there is strong supply of that type to the location through advection or mixing). Such circumstances may occur in highly energetic regions where there is a constant advected supply of different types (e.g. a fast moving Western Boundary Current). A highly varying set of environmental conditions will also help in this situation. For instance if μ_{max} is assumed to have temperature mediated
670 component (as in the numerical model, Supplemental text S1.1, Eq. S1.4), then many different types would have temporarily the "best" environment. However, these beneficial conditions may not occur often enough or long enough to maintain co-existence without the constant supply of new population. This is the situation in the hot spots of diversity seen in the default experiment, but which disappear in the experiment with no advection (Fig 11). See more discussion in Clayton et al., (2014).

We note that the hotspots do not appear in either the size class or functional group richness, suggesting that the temporal "best"

675 environment can be provided by varying temperatures, but no such temporary optimal situation occur in these circumstances for the other dimensional controls

Supplemental link

680 https://doi.org/10.7910/DVN/KXABE6

Author Contribution

S.D. conceived the experimental design, conducted the biogeochemical/ecosystem/optical model simulations, and performed most of the analysis. O.J. was responsible for the numerical code, with input from A.H. on the phytoplankton absorption

685 (Supplemental Fig S1). P.C. provided the Atlantic Meridional Transect observational data (Fig 1, 5, Supplemental Fig S6, S7). B.W. and M.J.F. provided input on the theoretical interpretations. B.W. provided schematic in Fig 2. DT provided input on the grazing parameterizations and the data for Supplemental Fig S2. S.D. led the writing with input from all authors.

Competing interests

690

The authors declare that they have no conflict of interest.

Acknowledgements

SD, MJF, OJ received funding from NASA (grants NNX16AR47G, 80NSSC17K0561). This work was also supported by the

695 Simons Collaboration on Computational Biogeochemical Modeling of Marine Ecosystems (CBIOMES) (Grant Id:549931).

References

Acevedo-Trejos, E., Marañón, E., and Merico, A: Phytoplankton size diversity and ecosystem function relationships across oceanic regions. Proc. R. Soc. B., 285, 20180621, doi: 10.1098/rspb.2018.0621, 2018.

700 Acevedo-Trejos, E., Brandt, G., Bruggeman, J., and Merico, A.: Mechanisms shaping size structure and functional diversity og phytoplankton communities in the ocean. Scientific Reports, 5, 8918, 2015.

Agawin, N.S.R., Rabouille, S., Veldhuis, M.J.W., Servatius, L., Hol, S., van Overzee, H.M.J., and Huisman J.: Competition and facilitation between unicellular nitrogen-fixing cyanobacteria and non-nitrogen-fixing phytoplankton species. Limnol. Oceanogr.52, 2233–2248, 2007.

705 Agawin, N. S. R., and. Agustí, S: Abundance, frequency of dividing cells and growth rates of *Synechococcus*sp. (cyanobacteria) in the stratified Northwest Mediterranean Sea. J. Plankton Res. 19, 1599–1615, 1997.

Allen, A.P., Gillooly, J.F. and Brown, J.H: Recasting the species–energy hypothesis: the different roles of kinetic and potential energy in regulating biodiversity. *Scaling biodiversity* (ed. by D. Storch, P.A. Marquet and J.H. Brown), pp. 283–299. Cambridge University Press, Cambridge, 2007.

710 Armstrong, R. A.: Grazing limitation and nutrient limitation in marine ecosystems: steady state solutions of an ecosystem model with multiple food chains. Limnol. Oceanogr., 39, 597–608, 1994.

Baird, M.E., One, R.R., Suthers, I.M., & Middleton, J.H.: A plankton population model with biomechanics descriptions of biological processes in an idealized 2D ocean basin. J. Mar, Sys. 50, 199-222, 2004.

Barton, A.D., Dutkiewicz, S., Flierl, G., Bragg, J. and Follows, M.J.: Patterns of Diversity in Marine Phytoplankton. Science, 715 327, 5972, 10.1126/science.1184961, 2010.

Barton, A.D., Irwin, A.J., Finkel, Z.V., and Stock, C: Anthropogenic climate change drives shift and shuffle in North Atlantic phytoplankton communities. Proceedings of the National Academy of Sciences USA 113, 2964-2969, 2016.

Barton, A.D., Finkel, Z.V., B.A. Ward, Johns, D.G. and Follows, M.J: On the roles of cell size and trophic strategy in North Atlantic diatom and dinoflagellate communities, Limnol. Oceanogr., 58, 254–266, doi:10.4319/lo.2013.58.1.0254, 2013.

720 Beardall, J., Allen, D., Bragg, J., Finkel, Z.V.,Flynn, K.J., Quigg, A.,Rees, T.A.V., Richardson, A., and Raven, J.A.: Allometry and stoichiometry of unicellular, colonial and multicellular phytoplankton. New Phytologist, Tansley Review, 2008.

Bec, B., Collos, Y., Vaquer, A.,Mouillot, D., and Sourchu, P.: Growth rate peaks at intermediate cell size in marine photosynthetic picoeukaryotes. Limnol. Oceanogr., 53, 863–867, 2008.

Bergman, B., Sandh, G., Lin, S., Larsson, J., and Carpenter E.J.:*Trichodesmium* – a widespread marine cyanobacterium with 725 unusual nitrogen fixation properties. FEMS Microbiol. Review, 37, 286-302, 2013.

Bissenger, J.E., Montagnes, D.J.S., Harples, J., and Atkinson, D.: Predicting marine phytoplankton maximum growth rates from temperature: Improving on the Eppley curve using quantile regression,Limnol. Oceangr.,53, 487-493, 2008.

Boatman, T.G., Lawson, T., and Geider, R.J.: A key marine diazotroph in a changing ocean: The interacting effects of temperature, CO2 and light on the growth of *Trichodesmium erythraeum* IMS101. PLOS ONE, 12, e0168796, doi:10.1371/journal.pone.0168796, 2017.

Boyd P., Rynearson, T.A., Evelyn A. Armstrong E.A.[1], Feixue Fu[4], Kendra Hayashi[5],

Zhangxi Hu[6], David A. Hutchins, D.A., Kudela[5], R.M., Litchman, E., Mulholland, M.R., Passow, U., Strzepek, R.F., Whittaker, K.A., Yu, E., Thomas M.K.: Marine phytoplankton temperature versus growth response from polar to tropical waters – outcome of a scientific community-wide study. PlosOne, 8, e63091, 2013.

Breitbarth, E., Wohler, J., Klas, J., LaRoche, J.,and Peekan, I.: Nitrogen fixation and growth rates of *Trichodesmium* IMS101 as a function of light intensity. Mar Ecol Prog Ser, 359, 25-36, 2008.

Buitenhuis E.T., Pangerc, T., Franklin, D.J., Le Quere, C., and Malin G.: Growth rates of six coccolithophorid strains as a function of temperature. Limnol. Oceanogr., 53, 1181-1185, 2008.

Buitenhuis, E. T., Li, W. K. W., Vaulot, D., Lomas, M. W., Landry, M. R., Partensky, F., Karl, D. M., Ulloa, O., Campbell, L., Jacquet, S., Lantoine, F., Chavez, F., Macias, D., Gosselin, M., and McManus, G. B.: Picophytoplankton biomass distribution in the global ocean, Earth Syst. Sci. Data, 4, 37–46, doi:10.5194/essd-4-37-2012, 2012.

Buitenhuis, E.T. Vogt, M., Moriarty, R., Bednaršek, N., Doney, S.C., Leblanc, K., Le Quéré, C., Luo, Y.-W., O'Brien, C., O'Brien, T., Peloquin, J., Schiebel, R. and Swan, C.: MAREDAT: towards a world atlas of MARine Ecosystem DATaEarth Syst. Sci. Data, 5, 227-239, 2013.

Busseni, G: Exploring diatom functional and taxonomic diversity on a global scale through an integrative approach. Doctoral Dissertation, The Open University and Statione Zoologica Anton Dohrn Napoli, 2018.

Cardinale, B. J., Matulich, K. L., Hooper, D. U., Byrnes, J. E., Duffy, E., Gamfeldt, L., Balvanera, P., O'Connor, M. I., and Gonzalez, A.: The functional role of producer diversity in ecosystems, Am. J. Bot., 98, 572–592, doi:10.3732/ajb.1000364, 2011.

Cardinale, B.J., Hillebrand, H., Harpole, W.S., Gross, K., and Ptacnik, R.: Separating the influence of resource 'availability' from resource 'imbalance' on productivity diversity relationships. Ecol. Let, 12, doi: 10.1111/j.1461-0248.2009.01317.x , 2009.

Cermeño, P., Choucino, P., Fernández-Castro, B., Figueiras, F.G., Marañón, E., Marrasé, C., Mouriño-Carballido, B., Pérez-Lorenzo, M., Rodríguez-Ramos, T., Teixeira, I.G. and Vallina, S.M.: Marine Primary Productivity Is Driven by a Selection Effect. Front. Mar. Sci. 3:173. doi: 10.3389/fmars.2016.00173, 2016.

Cermeño, P., Rodriguez-Ramos, T., Dornelas, M., Figueiras, F., Marañón, E., Teixeira, I.G. and Vallina, S.M. Species richness in marine phytoplankton communities is not correlated to ecosystem productivity. Mar. Ecol. Prog. Series, 488, doi: 10.3354/meps10443, 2013.

Cermeño, P., S. Dutkiewicz, S., Falkowski, P.G., Follows, M.J., Harris, R.P., and Schofield, O.: The role of oceanic nutricline depth in regulating Earth's carbon cycle. Proc Nat Academy of Sciences, 105, doi:10.1073/pnas.0811302106, 2008.

Chaudhary, C., Saeedi, H., and Costello, M.J.: Bimodality of latitudinal gradients in marine species richness. Trends in ecology & evolution 31, 670–676, 2016.

Chust, G., Irigoien, X., Chave, J., and Harris, R.P.: Latitudinal phytoplankton distribution and the neutral theory of biodiversity. Global Ecology and Biogeography, 22, 531–543, 2013.

Clayton S., Dutkiewicz, S., Jahn, O., and Follows, M. J.: Dispersal, eddies, and the diversity of marine phytoplankton. Limno. Oceanogr.: Fluids and Environments, 3, 182-197, 2013.

Clayton, S. Dutkiewicz, O. Jahn, C.N. Hill, P. Heimbach, and M.J. Follows. Biogeochemical versus ecological consequences of modeled ocean physics. Biogeosciences, 14, 2877-2889, 2017.

Christaki, U., Jacquet, S., Dolan, J.R., Vaulot, D., and Rassoulzadegan, F.: Differential grazing and growth on *Prochlorococcus* and *Synechococcus*by two contrasting ciliates. Limnol Oceanogr. 44, 52–61, 1999.

de Vargas, C., Audic, S., Henry, N., Decelle, J., Mahé, F., Logares, R., Lara, E., Berney, C., Le Bescot, N., Probert, I., Carmichael, M., Poulain, J., Romac, S., Colin, S., Aury, J.-M., Bittner, L., Chaffron, S., Dunthorn, M., Engelen, S., Flegontova, O., Guidi, L., Horák, A., Jaillon, O., Lima-Mendez, G., Lukeš, J., Malviya, S., Morard, R., Mulot, M., Scalco, E., Siano, R., Vincent, F., Zingone, A., Dimier, C., Picheral, M., Searson, S., Kandels-Lewis, S., Tara Oceans Coordinators, Acinas, S.G. Bork, P., Bowler, C., Gorsky, G., Grimsley, N., Hingamp, P., udicone, D., Not, F., Ogata, H., Pesant, S., Raes, J., Sieracki, M.E., Speich, S., Stemmann,L., Sunagawa, S., Weissenbach, J., Wincker, P., Karsenti, E.: Eukaryotic plankton diversity in the sunlit ocean. Science, 348, doi:10.1126/Science.1261605, 2015.

Dutkiewicz, S., Hickman, A.E., Jahn, O., Gregg, W.W., Mouw, C.B., and Follows, M.J.: Capturing optically important constituents and properties in a marine biogeochemical and ecosystem model. Biogeoscience, 12, 4447-4481 doi:10.5194/bg-12-4447-2015, 2015a.

Dutkiewicz, S., J. Morris, J., Follows, M.J., Scott, J., Levitan, O., Dyhrman, S., and Berman-Frank, I: Impact of ocean acidification on the structure of future phytoplankton communities.Nature Climate Change, doi:10.1038/nclimate2722, 2015b.

Dutkiewicz, S., Ward, B.A., Scott, J., and M. Follows, M.J.: Understanding predicted shifts in diazotroph biogeography using resource competition theory. Biogeoscience, 11, 5445-5461, doi:10.5194/bg-11-5445-2014, 2014.

Dutkiewicz, S., Ward, B.A., Monteiro, F., and Follows, M.J.: Interconnection between nitrogen fixers and iron in the Pacific Ocean: Theory and numerical model. Global Biogeochemical Cycles, 26, GB1012, doi:10.1029/2011GB004039, 2012.

Dutkiewicz, S., Follows, M.J., and Bragg, J.G.: Modeling the coupling of ocean ecology and biogeochemistry, Global Biogeochemical Cycles, 23, GB4017, doi:10.1029/2008GB003405, 2009.

Edwards K.F., Thomas M.K., Klausmeier C.A., and Litchman E.: Allometric scaling and taxonomic variation in nutrient utilization traits and maximum growth rate of phytoplankton. Limnol Oceanogr 57, 554–566, 2012.

Edwards, K. F., Klausmeier C.A., and Litchman. E.: Evidence for a three-way trade-off between nitrogen and phosphorus competitive abilities and cell size in phytoplankton. Ecology 92, 2085–2095, 2011.

Eppley, R. W.: Temperature and phytoplankton growth in the sea, Fish. B., 70, 1063–1085, 1972.

Falkowski, P.G., Barber, R.T., and Smetacek, V.: Biogeochemical controls and feedback on ocean primary production. Science, 281, 200-206, doi:10.1126/science.281.5374.200, 1998.

Fenchel, T.M. *Ecology of Protozoa*, Springer Berlin Heidelberg, p 187, 1987

Finkel, Z., and Irwin, A.J.: Modeling size-dependent photosynthesis: light absorption and the allometric rule. J. theor. Biol. 204: 361-369. 10.1006/jtbi.2000.2020, 2000.

Finkel, Z. V., Beardall, J., Flynn, K.J., Quigg, A., Rees, T.A.V., and Raven, J.A.: Phytoplankton in a changing world: cell size and elemental stoichiometry. J. Plankton Res. 32, 119–137, 2010.

Follows, M.J, Dutkiewicz, S., Ward, B.A., and Follett, C.N. Theoretical interpretation of subtropical plankton biogeography. In *Microbial Ecology of the Oceans*, 3rd Edition, Editors, J. Gasol, D Kirshman. Hoboken, NJ, John Wiley, p. 467, 2018.

Fuhrman J.A.: Microbial community structure and its functional implications. Nature 459, 193–199, 2009.

Follett, C.L., Dutkiewicz, S., Karl, D.M.Inomura, K., and M. Follows, M.J.: Why is there a summertime bloom of diatom-diazotroph associations in the North Pacific subtropical gyre? ISME Journal, doi:10.1038/s41396-017-0012-x, 2018.

Garcia, N.S, and Hutchins, D.A.: Light-limited growth rates modulate nitrate inhibition of dinitrogen fixation in the marine unicellular cyanobacterium *Crocosphaera watsonii.* PLOS ONE, 9, e114465, doi:10.1371/journal.pone.0114465, 2014.

Geider, R. J., MacIntyre, H. L., and Kana, T. M.: A dynamic regulatory model of photoacclimation to light, nutrient and temperature, Limnol. Oceanogr., 43, 679–694, 1998.

Grover, J.P.: Dynamics of competition among microalgae in variable environments: experimental test of alternative models. Oikos, 62, 231-243, 1991a.

Grover, J.P.: Resource competition in a variable environment: phytoplankton growing according to the variable-internal-stores model. Am. Nat., 138, 811-835, 1991b.

Guidi L, Stemmann L, Jackson GA, Ibanez F, Claustre H, Legendre, L., Picheral, M., and Gorsky, G.: Effects of phytoplankton community on production, size and export of large aggregates: a world-ocean analysis. Limnol. Oceanogr. 54, 1951–63, 2009.

Hansen, B.B., Bjornsen, B.W., and Hansen, P.J.: Zooplankton grazing and growth: Scaling within the 2– 2000 mm body size range. Limnol. Oceanogr. 42, 687–704, doi:10.4319/lo.1997.42.4.0687, 1997.

Hickman, A.E., Dutkiewicz, S., Williams, R.G., and Follows, M.J.: Modelling the effects of chromatic adaptation on phytoplankton community structure in the oligotrophic ocean. Marine Ecology Progress Series, 406, 1-17, doi:10.3354/meps08588, 2010.

Hillebrand, H.: On the generality of the latitudinal diversity gradient. The American Naturalist, 163, 192–211, 2004.

Hillebrand, H. and Azovsky, A.I.: Body size determines the strength of the latitudinal diversity gradient. Ecography, 24, 251–256, 2001.

Holling, C. S.: Some characteristics of simple types of predation and parasitism, Canadian Entomologist, 91, 385-398, 1959.

Huisman, J., and Weissing, F.J.: Light-limited growth and competition for light in well mixed aquatic environments: An elementary model. Ecology 75, 507–520, 1994.

Hutchins, D. A., Fu F.X., Zhang Y., Warner M.E., Feng, Y., Portune K., Bernhardt P.W., and Mulholland, M.R.: CO2 control of *Trichodesmium* N-2 fixation, photosynthesis, growth rates, and elemental ratios: Implications for past, present, and future ocean biogeochemistry. Limnol. Oceanogr, 52(4): 1293-1304. Doi:10.4319/lo.2007.52.4.1293, 2007.

830 Hutchinson, G.E.: The paradox of the plankton. Am. Nat., 95, 137-145, 1961.

Irigoien, X., Huisman, J. and Harris, R.P.: Global biodiversity patterns of marine phytoplankton and zooplankton. Nature, 429, 863–867, 2004.

Jeong, H.J., Yoo Y.D., Kim, J.S., Seon K.A., Kang, N.S., and Kim, T.H.: Growth, Feeding and Ecological Roles of the Mixotrophic and Heterotrophic Dinoflagellates in Marine Planktonic Food Webs. Ocean Sci. J. 45, 65-91, doi:

835 10.1007/s12601-010-0007-2, 2010.

Johnson, R., Strutton, P.G., Wright, S.W., McMinn, A., and Meiners, K.M.: Three improved Satellite Chlorophyll algorithms for the Southern Ocean, J. Geophys. Res. Oceans, 118, doi:10.1002/jgrc.20270, 2013

Johnson, Z.I, and Martiny, A.C.: Techniques for quantifying phytoplankton biodiversity, Ann Rev Mar Sci. 7, 299-324. doi: 10.1146/annurev-marine-010814-015902, 2015.

840 Johnson, Z. I., Zinser, E.R., Coe, A., McNulty, N.P., Woodward, E.M.S., Chisholm, S.W.: Niche partitioning among *Prochlorococcus* ecotypes along ocean-scale environmental gradients. Science,311, 1937–1740, 2006.

Kiorboe, T.: Turbulence, phytoplankton cell size, and the structure of pelagic food webs. Adv. Mar. Biol. 29, 1–72, doi:10.1016/S0065-2881(08)60129-7, 1993.

Kiorboe, T. *A mechanistic approach to plankton ecology.* Princeton University Press. 224 pp, 2008.

845 Kooijman, S.A.L.M. *Dynamic Energy and Mass Budget in Biological Systems*, Cambridge Univ. Press, 2000.

Kranz, S.A., Levitan, O., Richter, K.-U., Prasil, O., Berman-Frank, I. and Rost, B:. Combined effect of CO2 and light on the N2-fixing cyanobacterium *Trichodesmium* IMS101: Physiological responses. Plant Physiol., 154, 334-345, doi:10.1104.pp.110.159145, 2010.

Kremer, C.T. and Klausmeier, C.A.: Species packing in eco-evolutionary models of seasonally fluctuating environments, Ecol.

850 Let, 20, 1158-1168, doi: 10.1111/ele.12813, 2017.

Lampert, W.: Zooplankton research: the contribution of limnology to general ecological paradigms. Aquatic Ecologu, 31, 19-27, 1997.

Leblanc, K., Arístegui, J., Armand, L., Assmy, P., Beker, B., Bode, A., Breton, E., Cornet, V., Gibson, J., Gosselin, M.-P., Kopczynska, E., Marshall, H., Peloquin, J., Piontkovski, S., Poulton, A. J., Quéguiner, B., Schiebel, R., Shipe, R., Stefels, J.,

855 van Leeuwe, M. A., Varela, M., Widdicombe, C., and Yallop, M.: A global diatom database – abundance, biovolume and biomass in the world ocean, Earth Syst. Sci. Data, 4, 149–165, doi:10.5194/essd-4-149-2012 (2012)

Lévy, M., Jahn, O., Dutkiewicz, S., and Follows, M. J.: Phytoplankton diversity and community structure affected by oceanic dispersal and mesoscale turbulence. Limno. Oceanogr.: Fluids and Environments, 4, 67-84, 2014.

Lévy, M., Jahn, O., Dutkiewicz, S., Follows, M.J., and d'Ovidio, F.: The dynamical landscape of marine phytoplankton

860 diversity. Journal of Royal Society Interface, 12, 20150481, 2015.

Lewandowska, A.M. Biermann, A.,Borer, E.T., Cebrian-Piqueras, M.A., Declerck, S.A.J., De Meester, L., Van Donk, E., Gamfeldt, L., Gruner, D.S., Hagenah, N., Harpole, W.S., Kirkman, K.P., Klausmeier, C.A., Kleyer, M., Knops, J.M.H., Lemmens, P., Lind, E.M., Litchman, E., Mantilla-Contreras, J., Martens, K., Meier, S., Minden, V., Moore, J.L., Olde Venterink, H., Seabloom, E.W., Sommer, U., Striebel, M.,Trenkamp, A., Trinogga, J., Urabe, J., Vyverman, W., Van de Waal,

865   D.B., Widdicombe, C.E., and Hillebrand, H.: The influence of balanced and imbalanced resource supply on biodiversity – functioning relationship across ecosystems. Phil. Trans. R. Soc. B 371: 20150283. http://dx.doi.org/10.1098/rstb.2015.0283, 2016.

Lima-Mendez, G., Faust, K., Henry, N.C., Decelle, J., Colin, S., Carcillo, F., Chaffron, S., Ignacio-Espinosa, J.C., Roux, S., Vincent, F.J., Bittner, L., Darzi, Y., Wang, J., Audic, S., Berline, L., Bontempi, G., Cabello, A.M., Coppola, L., Cornejo-

870   Castillo, F.M., d'Ovidio, F.D., Meester, L.D., Ferrera, I., Garet-Delmas, M., Guidi, L., Lara, E., Pesant, S., Royo-Llonch, M., Salazar, G., Sánchez, P., Sebastián, M.G., Souffreau, C., Dimier, C., Picheral, M., Searson, S., Kandels-Lewis, S., Gorsky, G., Not, F., Ogata, H., Speich, S., Stemmann, L., Weissenbach, J., Wincker, P., Acinas, S.G., Sunagawa, S., Bork, P., Sullivan, M.B., Karsenti, E., Bowler, C., Vargas, C.D., and Raes, J.: Determinants of community structure in the global plankton interactome. Science, 22, 348(6237):1262073. doi: 10.1126/science.1262073, 2015.

875   Litchman, E., de Tezanos Pinto, P., Klausmeier, C.A., Thomas, M.K., Yoshiyama, K.: Linking traits to species diversity and comminuty structure in phytoplankton. Hydrobiologia, 653, 15-28, doi: 10.1007/s10750-010-0341-5, 2010.

Luo, Y.-W., Doney, S. C., Anderson, L. A., Benavides, M., BermanFrank, I., Bode, A., Bonnet, S., Boström, K. H., Böttjer, D., Capone, D. G., Carpenter, E. J., Chen, Y. L., Church, M. J., Dore, J. E., Falcón, L. I., Fernández, A., Foster, R. A., Furuya, K., Gómez, F., Gundersen, K., Hynes, A. M., Karl, D. M., Kitajima, S., Langlois, R. J., LaRoche, J., Letelier, R. M., Marañón,

880   E., McGillicuddy Jr., D. J., Moisander, P. H., Moore, C. M., Mouriño-Carballido, B., Mulholland, M. R., Needoba, J. A., Orcutt, K. M., Poulton, A. J., Rahav, E., Raimbault, P., Rees, A. P., Riemann, L., Shiozaki, T., Subramaniam, A., Tyrrell, T., Turk-Kubo, K. A., Varela, M., Villareal, T. A., Webb, E. A., White, A. E., Wu, J., and Zehr, J. P.: Database of diazotrophs in global ocean: abundance, biomass and nitrogen fixation rates, Earth Syst. Sci. Data, 4, 47–73, doi:10.5194/essd-4-47-2012, 2012.

885   Marañón, E., Cermeño, P., López-Sandoval, D.C., Rodríguez-Ramos, T., Sobrino, C., Huete-Ortega, M., Blanco, J.M. and Rodríguez, J.: Unimodal size scaling of phytoplankton growth and the size dependence of nutrient uptake and use. Ecology Letters 16, 371–379, 2013.

Marañón E, Cermeño P, Latasa M, and Tadonléké, R.D.: Resource supply alone explains the variability of marine phytoplankton size structure. Limno. Oceanogr. 60, 1848-1854, doi:10.1002/lno.10138, 2015.

890   Margalef, R.: Life-forms of phytoplankton as survival alternatives in an unstable environment. Oceanol Acta 1: 493−509, 1978.

Marshall, J., Adcroft, A., Hill, C.N., Perelman, L., and Heisey, C.: A finite-volume, incompressible Navier–Stokes model for studies of the ocean on parallel computers, J. Geophys. Res., 102, 5753–5766, 1997.

Matthiessen B. and Hillebrand, H.: Dispersal frequency affect local biomass production by controlling local diversity. Ecol. Letters, 9 652-662, doi:10.111/j.1461-0248.2006.00915.x, 2006.

McCann K.: The diversity-stability debate. Nature,405, 228–33, 2000.

Miller, T. E.H. Burns, J.H., Munguia, P., Walters, E.L.,Kneitel, J.M., Richards, P.M., Mouquet, N., and Buckley, H.L.: A critical review of twenty years use of the resource-ratio theory. Am. Nat. 165, 439–448, 2005.

Monteiro, F.M., Bach, L.T., Brownlee, C., Brown, P., Rickaby, R.E.M., Tyrrell, T., Beaufort, L., Dutkiewicz, S., Gibbs, S., Gutowska, M.A., Lee, R., Poulton, A.J., Riebesell, U., Young, J., and Ridgwell, A.: Why marine phytoplankton calcify? Science Advances, 2, doi:0.1126/sciadv.1501822, 2016.

Moore, L. R., Rocap, G., and Chisholm, S.: Physiology and molecular phylogeny of coexisting *Prochorococcus*ecotypes. Nature 393, 464–46, 1998.

Moore, T.S., Campell, J.W., and Dowel, M.D.: A class-based approach to characterizing and mapping the uncertainty of the MODIS ocean chlorophyll product. Remote Sensing of Environment, 113, 2424–2430, 2009.

Morel, A., Ahn, Y.-H., Partensky, F., Vaulot, D., and Claustre, H.: *Prochlorococcus* and *Synechococcus*: A comparative study of their optical properties in relation to their size and pigmentation J. Mar. Res. 51, 617–649, 1993.

Mouriño-Carballido B., Hojas E., Cermeño P., Chouciño P. Fernández-Castro, B., Latasa, M., Marañón, E., Morán, X.A.G., Vida, M.: Nutrient supply controls picoplankton community structure during three contrasting seasons in the northwestern Mediterranean Sea. Mar Ecol Prog Ser 543, 1-19,19. doi:10.3354/meps11558, 2016.

Mousing, E.A., Richardson, K., Bendtsen, J., Cetinic, I., and Perry, M.J.: Evidence of small-scale spatil structuring of phytoplankton alpha- and beta-diversity in the open ocean. J. Ecology, 104, 1682-1695, doi:10.1111/1365-2745.12634, 2016.

O'Brien, C. J., Peloquin, J. A., Vogt, M., Heinle, M., Gruber, N., Ajani, P., Andruleit, H., Arístegui, J., Beaufort, L., Estrada, M., Karentz, D., Kopczynska, E., Lee, R., Poulton, A. J., Pritchard, T., and Widdicombe, C.: Global marine plankton functional type biomass distributions: coccolithophores, Earth Syst. Sci. Data, 5, 259–276, doi:10.5194/essd-5-259-2013, 2013.

Pančić, M., Rodriguez Torres, R., Almeda, R., and Kiørboe, T.:Silicified cell walls as a defensive trait in diatoms. Proceedings of the Royal Society B: Biological Sciences, 286, doi:10.1098/rspb.2019.0184, 2019.

Poulin, F.J., and Franks P.J.S.: Size-structured planktonic ecosystems: constraints, controls and assembly instructions. Journal of Plankton Research. 32:1121-1130, 2010.

Powell, M.G. and Glazier, D.S.: Asymmetric geographic range expansion explains the latitudinal diversity gradients of four major taxa of marine plankton, Paleobiology, 42, 196-208, doi: 10.1017/pab.2016.38, 2017.

Prowe, A.E.F., Pahlow, M., Dutkiewicz, S., Follows, M.J., and A. Oschlies, A.: Top-down control of marine phytoplankton diversity in a global ecosystem model. Progress in Oceanography, 101, 1-13, doi:10.1016/j.pocean.2011.11.016, 2012.

Ptacnik, R., Solimini, A.G., Andersen, T., Tamminsen, T., Brettum, P., Lepisto, L., Willen, E., Rekolainen, S.: Diversity predicts stability and resource use efficiency in natural phytoplankton communities. Proceeding Nat Acadamy, 105, 5134-5138, 2008.

Raven, J. A.: Why are there no picoplanktonic O2 evolvers with volumes less than 10^{-19} m³? Journal of Plankton Research 16, 65– 580, 1994.

Reich, P.B., Tilman, D., Isbell, F., Mueller, K., Hobbie, S.E., Flynn, D.F.B., and Eisenhauer, N.: Impacts of biodiversity loss excalates through time as redundancy fades, Science, 336, 589-592, doi:10.1126/science.1217909, 2012.

Righetti, D., Vogt, M., Gruber, N., Psomas, A., and Zimmermann, N.E.: Global patterns of phytoplankton diversity driven by temperature and environmental variability. Sci. Adv., 5, eaau6253, 2019.

Rodriguez-Ramos, M., Marañón, E., and Cermeno, P.: Marine nano- and microphytoplankton diversity: redrawing global patterns from sampling-standardized data. Global Ecol. Biogeogr., 24, 527-538, 2015.

Sal, S., López-Urrutia, Á., Irigoien, X., Harbour, D.S. and Harris, R.P.: Marine microplankton diversity database: ecological archives E094-149. Ecology, 94, 1658, 2013.

Sarthou, G., Timmermans, K.R., Blain, S., and Treguer, P.:Growth physiology and fate of diatoms in the ocean: A review. J. Sea Res. 53, 25–42, 2005.

Schade, J. D., Espeleta, J.F., Klausmeier, C.A., M. E. McGroddy, M.E., Thomas, S.A., and Zhang, L.: A conceptual framework for ecosystem stoichiometry: Balancingresource supply and demand. Oikos 109: 40–51, doi:10.1111/j.0030-1299.2005.14050.x, 2005.

Schartau, M.,Landry, M.R., and Armstrong, R.A. Density estimation of plankton size spectra: a reanalysis of IronEx II data, Journal of Plankton Research, 32, 8, 1167, 2010.

Shi, D., Kranz, S.A., Kim J.-M., and Morel, F.M.M.: Ocean acidification slows nitrogen fixation and growth in the dominant diazotroph Trichodesmium under low-iron conditions. Proc. Nat. Academy Sciences USA, doi:10.1073/pnas.1216012109, 2012.

Smith V.H.: Microbial diversity-productivity relationships in aquatic ecosystems. FEMS Microbial Ecol, 62, 181-186, doi:10.1111/j.1574-6941.2007.00381.x, 2007.

Snow, J. T., Schlosser, C., Woodward, E.M.S., Mills, M.M., Achterberg, E.P., Bibby, T.S., and Moore, C.M.: Environmental controls on the biogeography of diazotrophy and *Trichodesmium* in the Atlantic Ocean. GlobalBiogeochem. Cycles29, doi:10.1002/2015GB005090, 2015.

Sommer, U., Charalampous, E., Genitsaris, S., and Moustaka-Gouni, M.: Benefits, costs and taxonomic distribution of marine phytoplankton body size. J. Plankton Res., 39, 494-508, doi:10.1093/plankt/fbw071, 2017.

Sommer, U., Charalampous, E., Cotti, M., and Moustaka-Gouni, M.: Big fish eat small fish: Implications for food chain length? Community Ecology, 19,107-115, doi:10.1556/168.2018.19.2.2., 2018.

Sommer, U. Nitrate and silicate competition among Antarctic phytoplankton. *Mar. Biol.*91, 345–351, 1986.

Stramski, D., Bricaud, A., and Morel, A.: Modeling the inherent optical properties of the ocean based on the detailed composition of the planktonic community, Appl. Optics, 40, 2929–2945, 2001.

Tang, E.P.Y.: The allometry of algal growth rates. J. Plankton Res. 17 (6), 1325–1335, 1995.

960 Taniguchi, D.A.A., Landry, M.R., Franks, P.J.S. and Selph, K.E.: Size-specific growth and grazing rates for picophytoplankton in coastal and oceanic regions of the eastern Pacific. Marine Ecology Progress Series. 509, 87-101, 2014.

Terseleer, N., Bruggeman, J., Lancelot, C., and Gypens, N.: Trait-based respresentation of diatom functional diversity in a plankton functional type model of the eutrophied southern North Sea. Limnol. Oceanogr, 59, 1958-1972, doi:10.4319/lo.2014.59.6.1958, 2014.

965 Tilman, D.: Resource competition between planktonic algae: An experimental and theoretical approach, Ecology, 58, 338–348, 1977.

Tilman, D.: Resource Competition and Community Structure, Pop. Biol., vol. 17, 296 pp., Princeton Univ. Press, Princeton, N. J., 1982.

Thomas, M.K., Kremer C.T., Klausmeier C.A., and Litchman E.: A global pattern of thermal adaptation in marine
970 phytoplankton. Science, DOI: 10.1126/science.1224836, 2012.

Tréguer, P., Bowler, C., Moriceau, B., Dutkiewicz, S., Gehlen, M., Leblanc, K., Aumont, O., Bittner, L., Dugdale, R., Finkel, Z., Iudicone, D., Jahn, O., Guidi, L., Lasbleiz, M., Levy, M., and Pondaven, P.: Influence of diatoms on the ocean biological pump. Nature Geoscience, doi:10.1038/s41561-017-0028-x, 2017.

Vallina, S., Cermeno, P., Dutkiewicz, S., Loreau, M. and and Montoya, J.M.: Phytoplankton functional diversity increases
975 ecosystem productivity and stability. Ecological Modelling, 361, 18-1996, 2017.

Vallina, S.M., Follows, M.J., Dutkiewicz, S., Montoya, J., Cermeno, P. and Loreau, M.: Global relationship between phytoplankton diversity and productivity in the ocean. Nat. Comm., 5, 4299, doi:10.1038/ncomms5299, 2014b.

Vallina, S.M, Ward, B.A., Dutkiewicz, S., and Follows, M.J.: Maximal foraging with active prey-switching: a new "kill the winner" functional response and its effect on global species richness and biogeography. Prog. Oceanogr., 120, 93-109, 2014a.

980 Verdy, A. Follows, M., and Flierl, G.: Optimal phytoplankton cell size in an allometeric model. Mar Ecol Prog Ser, 379, 1-12, doi:10.3354/meps07909, 2009.

Ward B.A., Marañón E., Sauterey B., Rault J. and Claessen C.: The size-dependence of phytoplankton growth rates: a trade-off between nutrient uptake and metabolism. The American Naturalist, 189 (2), 170-177, 2017.

Ward B.A.: Temperature-Correlated Changes in Phytoplankton Community Structure Are Restricted to Polar Waters. PLOS
985 ONE, 10 (8): e0135581. doi:10.1371/journal.pone.0135581, 2015.

Ward, B.A., Dutkiewicz, S., and Follows, M.J.: Modelling spatial and temporal patterns in size-structured marine plankton communities: top-down and bottom-up controls. J. Plankton Res., 36, 31-47 doi:10.1093/plankt/fbt097, 2014.

Ward, B.A., Dutkiewicz, S., Moore, C.M., and Follows, M.J.: Iron, phosphorus and nitrogen supply ratios define the biogeography of nitrogen fixation. Limno. Oceanogr., 58, 2059-2075, 2013.

990 Ward, B.A., Dutkiewicz, S., Jahn, O., and Follows, M.J.: A size structured food-web model for the global ocean. Limnology and Oceanography, 57, 1877-1891, 2012.

Webb, E.A., Ehrenreich, I.M., Brown, S.L., Valois, F.W., and Waterbury, J.B.: Pheotypic and genotypic characterization of multiple strains of the diazotrophic cyanobacterium, *Crocosphaera watsonii*, isolated from the open ocean. Environ. Microbiol., 11, 338-348, 2009.

995 Weisse, T., Anderson, R., Arndt, H., Calbet, A., Hansen, P.J., Montagnes, D.J.S: Functional ecology of aquatic phagotrophic protists – Concepts , limitations , and perspectives, Eur. J. Protistol, 55, 50-74, doi:10.1016/j.ejop.2016.03.003, 2016.

Wilson, J. B., Spijkerman, E., and Huisman, J: Is there really insufficient support for Tilman's R* concept? A comment on Miller et al. Am. Nat.169: 700–706, 2007.

Wilson, S.T., Aylward, F.O., Ribalet, F., Benedetto, B., Case, J.R., Connell, P.E., Eppley, J.M., Ferran, S., Fitzsimmons, J.N.,
1000 Hayes, C.T., Romano, A.E., Turk-Kubo, K.A., Vislova, A., Armbrust, E.V., Carno, D.A., Church, M.J., Zehr, J.P., Karl, D.M., and DeLong, E.F.: Coordinated regulation of growth, activity and transcription in natural populations of the unicellular nitrogen-fixing cyanobacterium *Crocosphaera*. Nature Microbiol., 2, doi:10.1038/nmicrobiol.2017.118, 2017.

Worm, B., Hillebrand, H., and Sommer, U.: Consumer versus resource control of species diversity and ecosystem functioning, Nature, 417, 848-851, 2002.

1005 Wunsch C. and Heimbach, P.: Practical global ocean state estimation, Physica D, 230, 197-208, 2007.

	EXP-0	**EXP-1**	**EXP-2**	**EXP-3**
Number grazers	16	1	16	16
Nutrient requirements of functional groups	Differing	Differing	Same	Differing
Horizontal transport of plankton	Yes	Yes	Yes	No

Table of sensitivity experiments.
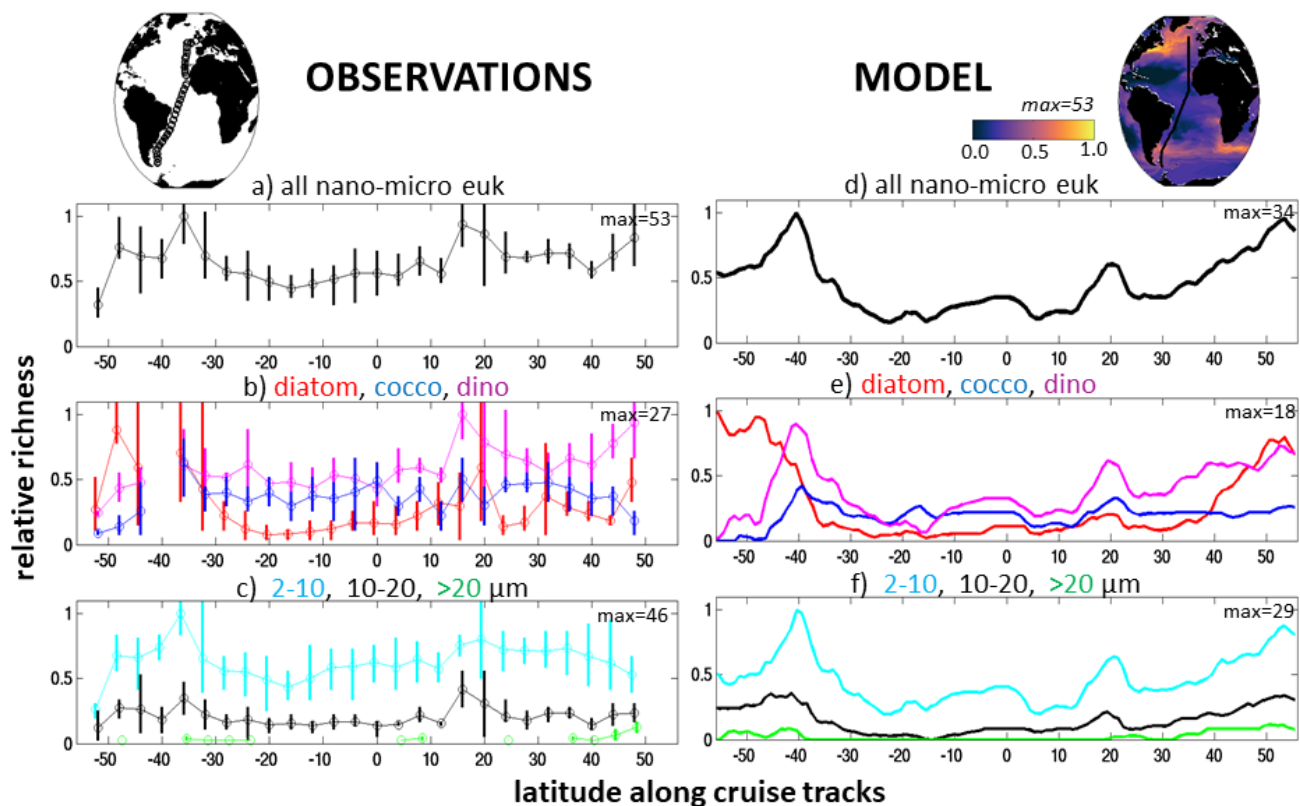
1015

Fig 1: Nano- and micro-eukaryote normalized richness in the Atlantic. Left: richness (number of co-existing species) normalized to the maximum along the Atlantic Meridional Transects (AMT) 1,2,3,4 for microscopy counts (see methods). Right: normalized annual mean richness from model. (a),(d) all diatoms, coccolithophores and dinoflagellates together; (b),(e) each functional groups separately (red: diatoms, dark blue: coccolithophores, purple: dinoflagellates); (c),(f) 3 size classes

1020 (light blue: 2-10µm, black: 10-20µm, green: <20µm). In left panels, circles are mean of four transects (2 in May, 2 in September) within 4° latitude bins, the vertical lines indicate the range within each bin. The maximum number used to normalise the plots are provided in each panel. Model pico-phytoplankton and diazotrophs are not included in the model analysis as they were not included in the observations. Maps show the cruise track of the AMTs, and for the model includes the annual mean normalized richness of the diatoms, coccolithophores and dinoflagellates together.

1025
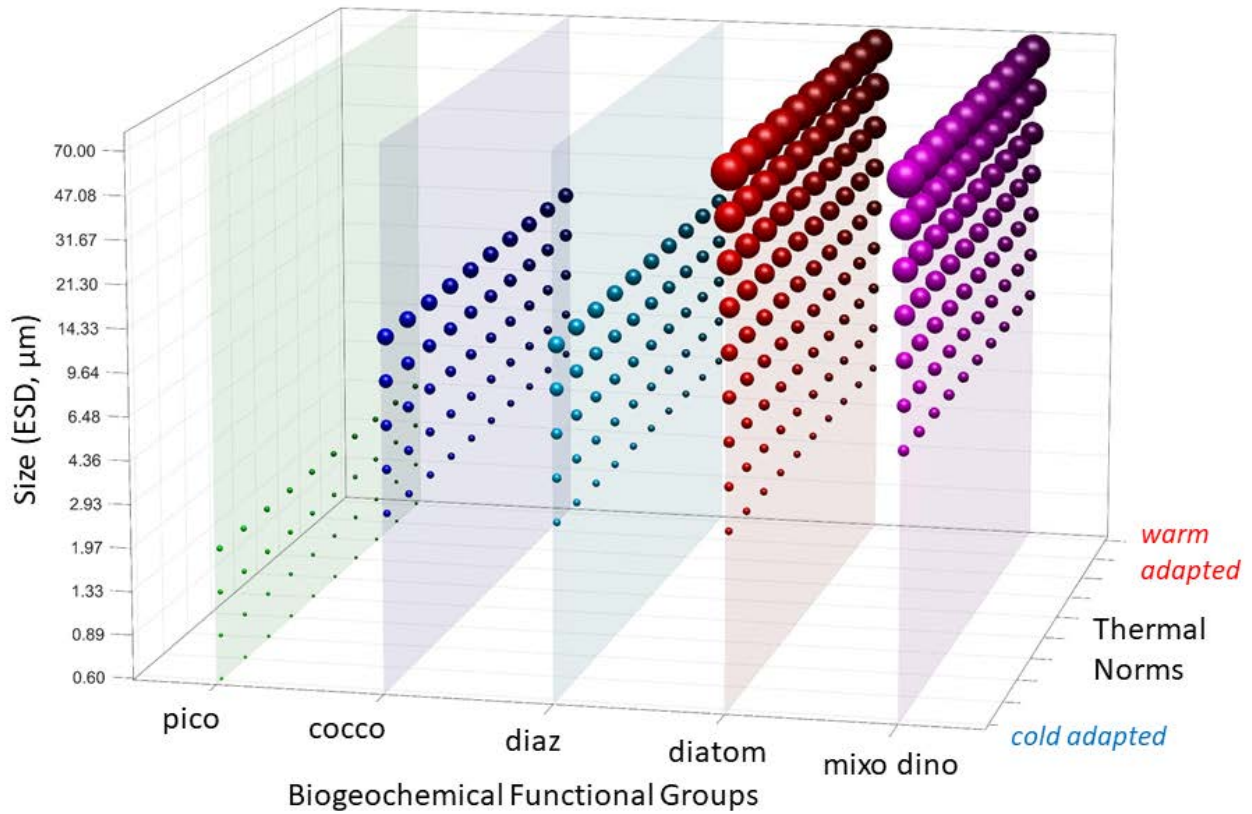
Figure 2: Schematic of the three dimensions of trait space: size classes, biogeochemical functional groups and thermal norms. There are 16 size classes, 5 functional groups and 10 thermal norms. In all there are 350 individual phytoplankton types. However, the 3 largest size classes go extinct, and as such here (and in other figures) we show only 13 size classes.
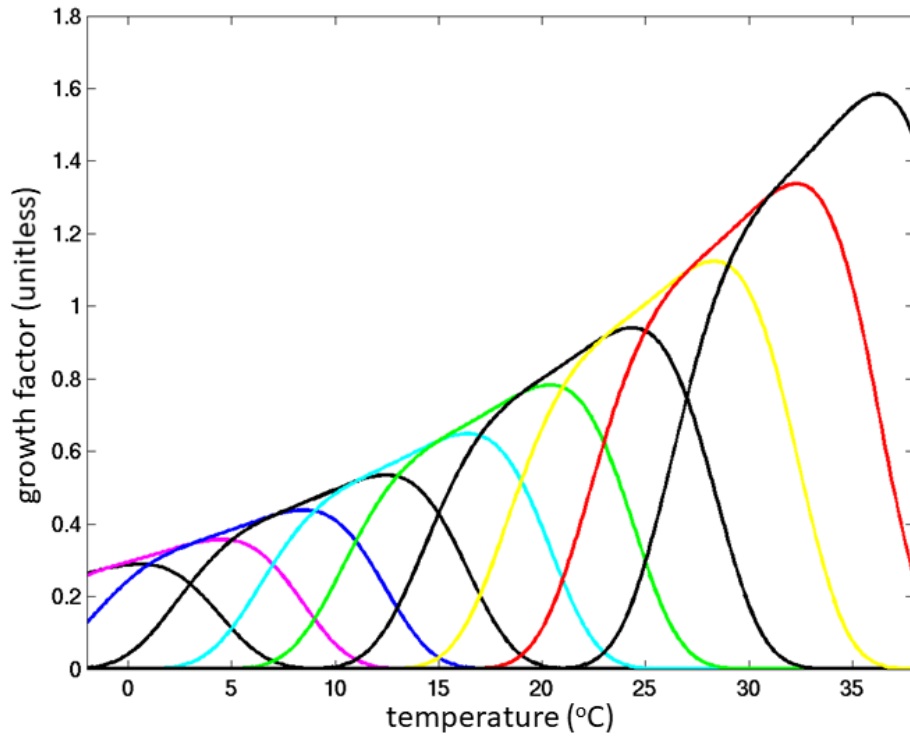
Figure 3: Growth as a function of temperature. Shown are the 10 thermal norms (unitless), each with a different colour. The function used here is from Dutkiewicz et al (2015b) and is discussed further in Supplemental material.
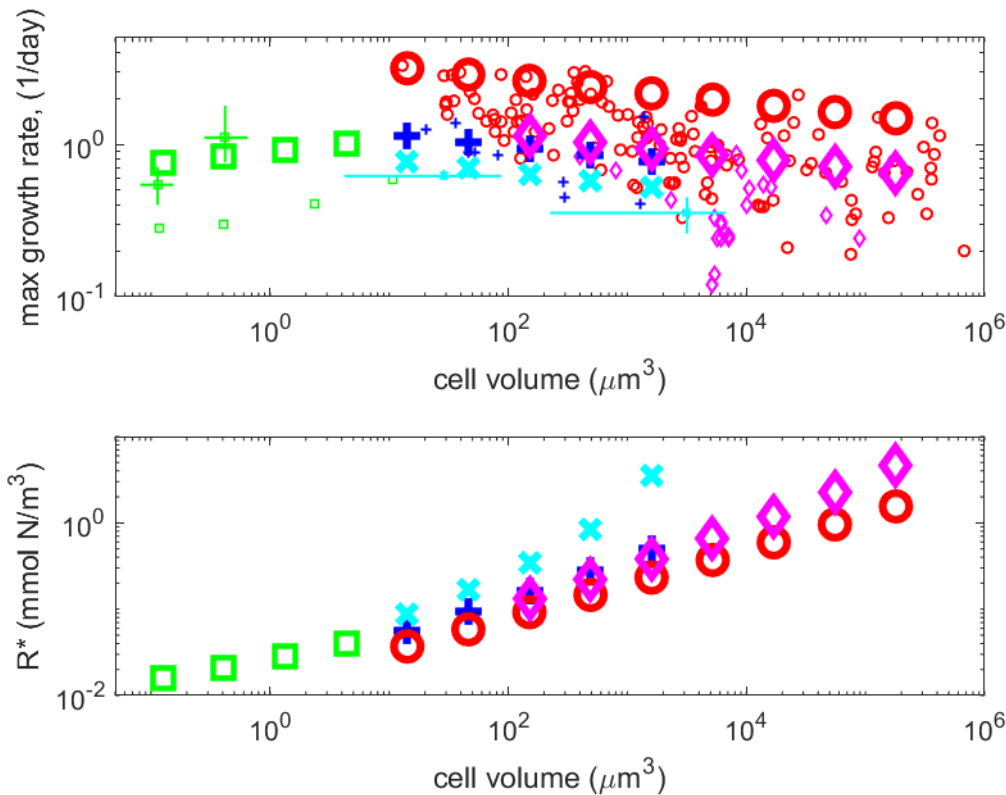
1035

Figure 4: Model Parameters guide by laboratory studies. Phytoplankton maximum growth rate (top) and R* (bottom) as a function of cell size. In (a) small symbols indicate laboratory studies normalized to 20º C, large symbols indicate the model size/functional groups. Colour of symbols denotes different functional groups: red circle=diatoms; purple diamond=mixotrophic dinoflagellates; dark blue plus=coccolithophores; light blue cross=diazotrophs; green square=pico-

1040 phytoplankton. In (b), $R^* = \frac{k_R M}{\mu_{max} - M}$, where M=0.5 1/d (see appendix). Data compilations of concurrent size and growth in (a) are from Tang (1995); Maranon et al. (2013); Sarthou et al (2005); Buitenhuis et al (2008). Additional data are derived from separate measurement of size and growth: These are shown as light lines centred at the mean and arms covering range. These are for the pico-prokaryotes (green) *Prochlorococcus* and *Synecochoccus* (Morel et al., 1993, Johnson et al. 2006, Christaki et al. 1999, Moore et al. 1998, Agawin and Agustí 1997) and the diazotrophs (light blue) *Crocosphaera* and *Trichodesmium*

1045 (Garcia and Hutchins, 2014; Webb et al, 2009; Wilson et al, 2017; Bergman et al, 2013; Boatman et al 2017; Beithbarth et al, 2008; Hutchins et al 2007; Kranz et al., 2010; Shi et al, 2012).
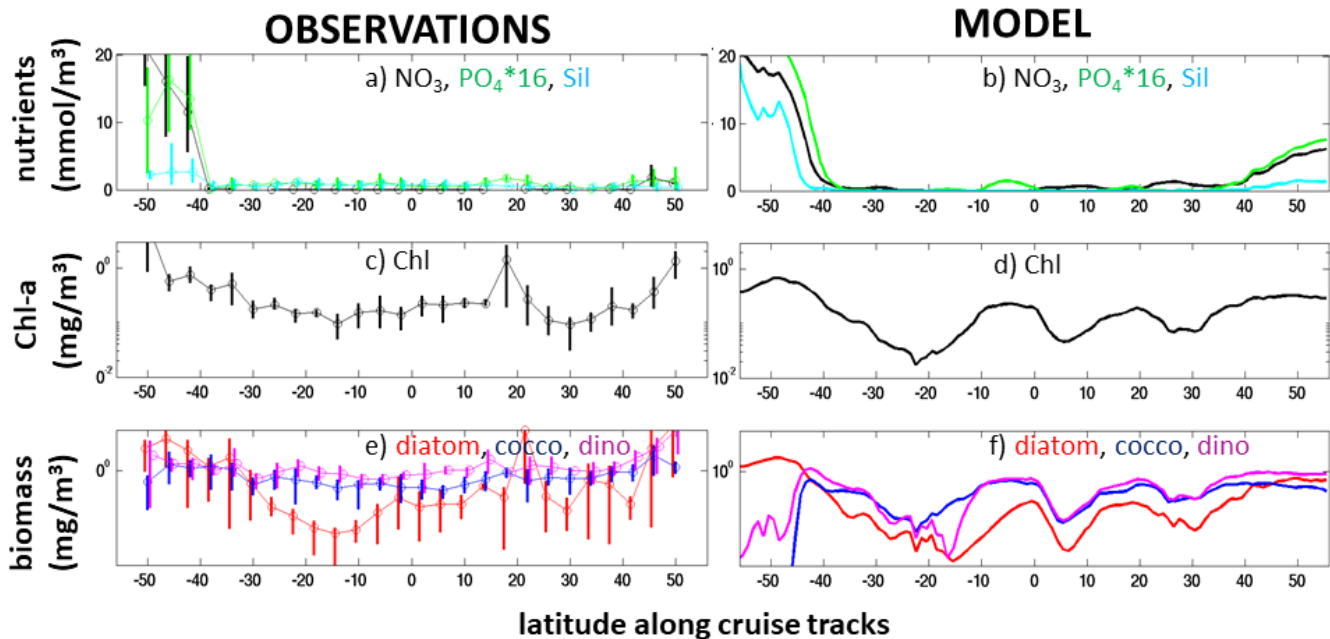
Figure 5: Observations and model output along the Atlantic Meridional Transect (AMT). (a), (b) nutrients (black=nitrate, mmolN/m^3; green=phosphate, x16 mmolP/m^3; light blue=silicic acid, mmolSi/m^3); (c), (d) Chl-a (mg Chl/m^3); (e), (f) phytoplankton biomass (mg C/m^3; red=diatoms; blue=coccolithophores; purple=dinoflagellates). Observations (left panels) are mean (circles) for the 4 AMT cruises (2 in May, 2 in September, see transects in Fig 1 maps) in 4° bins, the vertical lines show the range within each bin. Model results are annual mean along the AMT cruise track.
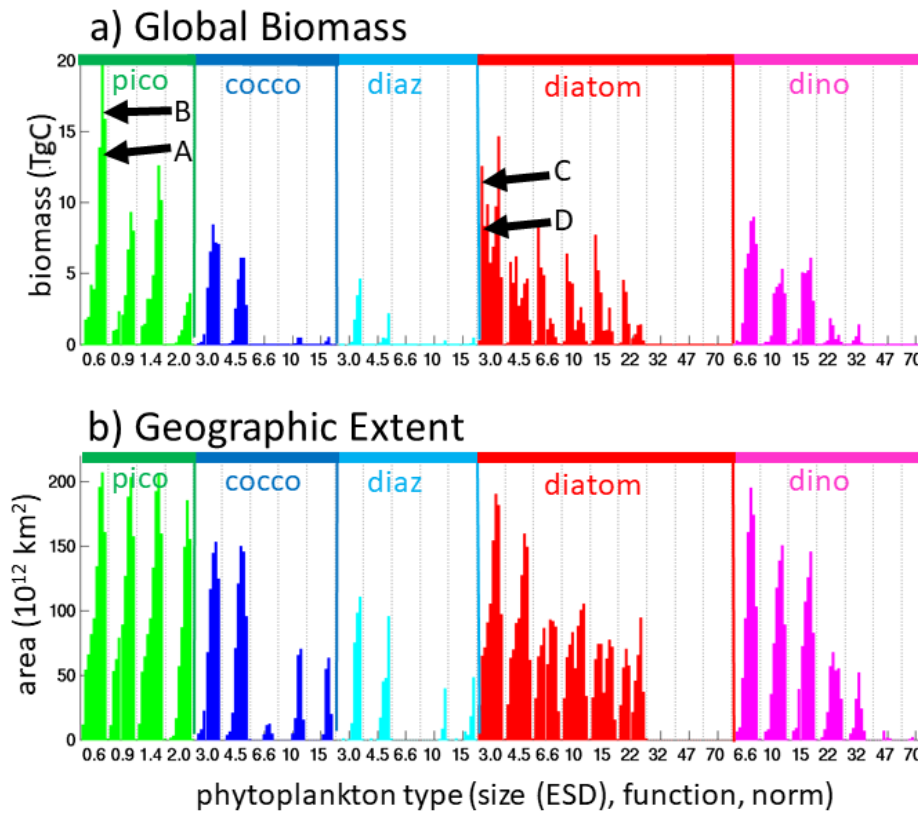
1060

Figure 6: Model phytoplankton types biomass and range. (a) Global integrated biomass (TgC); (b) Areal extent of the type (10^{12} km^2). Types are arranged by functional group as indicated by colour and labels at the top of the graph, by size classes (equivalent spherical diameter, ESD) as labelled below the graph, and thermal norms from cold adapted to warm adapted from left to right in between vertical dotted lines. The text (A,B,C,D) in panel (a) refers to representative types whose distributions

1065   are shown in Supplemental Fig S9.
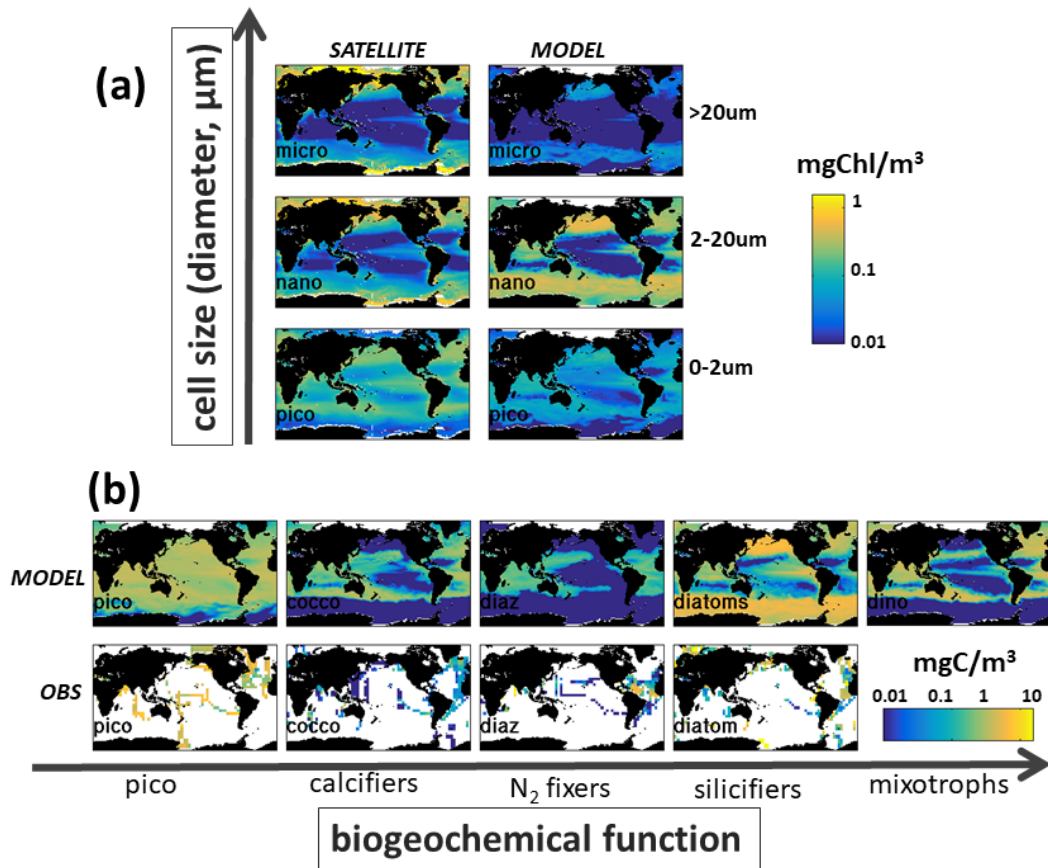
Figure 7. Comparison to Observations. (a) Sizes Classes: Chl-a concentration (mg Chl/m3) in pico (<2um), nano (2-20um) and micro (>20um) phytoplankton from (left) a satellite derived estimate (Ward, 2015) and (right) default model (0-50m); and (b) Functional groups (top) default model (0-50m) and (bottom) data compilation (MAREDAT, Buitenhuis et al 2013) in carbon biomass (mgC/m^3). Note the difference in units for (a) and (b), chosen to match the appropriate observations. For the MAREDAT databases: pico-phytoplankton (Buitenhuis et al 2012); coccolithophores (O'Brien et al 2013); diazotrophs (Lou et al 2012); diatoms (LeBlanc et al 2012). There was no MAREDAT dataset for dinoflagellates.
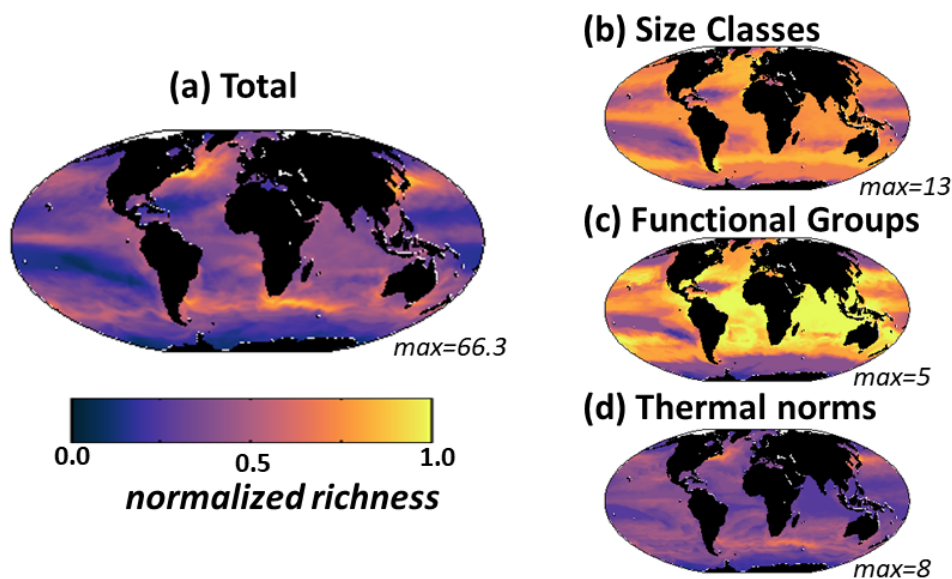
Figure 8: Model diversity measured as annual mean normalized richness in the surface layer. Normalization is by the maximum value for that plot (value noted bottom right of each panel)**.** (a) total richness determined by number of individual phytoplankton types that co-exist at any location; (b) size class richness determined by number of co-existing size classes; (c) functional richness determined by number of co-existing biogeochemical functional groups; (d) thermal richness determined by number of co-existing temperature norms. Total richness (a) is a (complex) multiplicative function of the three sub-richness categories (b-d). At first glance it may seem that thermal norm diversity (d) is most important, but this is only because our eyes are drawn to the hotspots. In reality, total diversity patterns (a) are strongly impacted by all three dimensions of diversity (see main text and sensitivity studies).
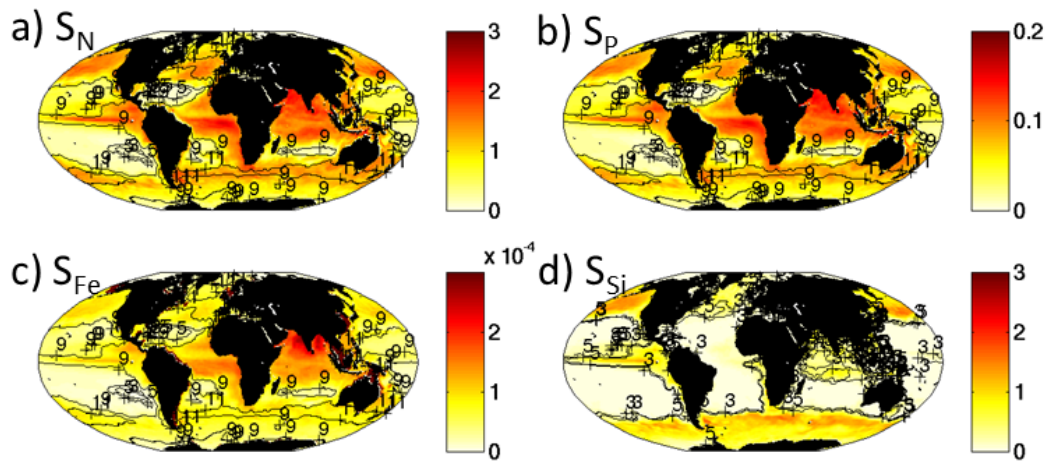
Figure 9: Model rate of supply of nutrients into top 50m. Supply rate of (a) Dissolved inorganic nitrogen (mol N/m^2/y); (b) Phosphate (mol P/m^2/y); (c) Iron (mol Fe/m^2/y); (d) Silicic acid (mol Si/m^2/y). All transport, diffusion and remineralization terms are included, and for iron also dust supply. In a-c, contours are size class richness from the total phytoplankton community (Fig. 4b), and in d contour is for size classes within diatom functional group alone. Since there are multiple limiting nutrients (especially for the non-diatoms), patterns of size diversity shown in a,b,c do not exactly match any single nutrient supply rate. However, the link between size classes of diatoms and silicic acid supply are clear in d.
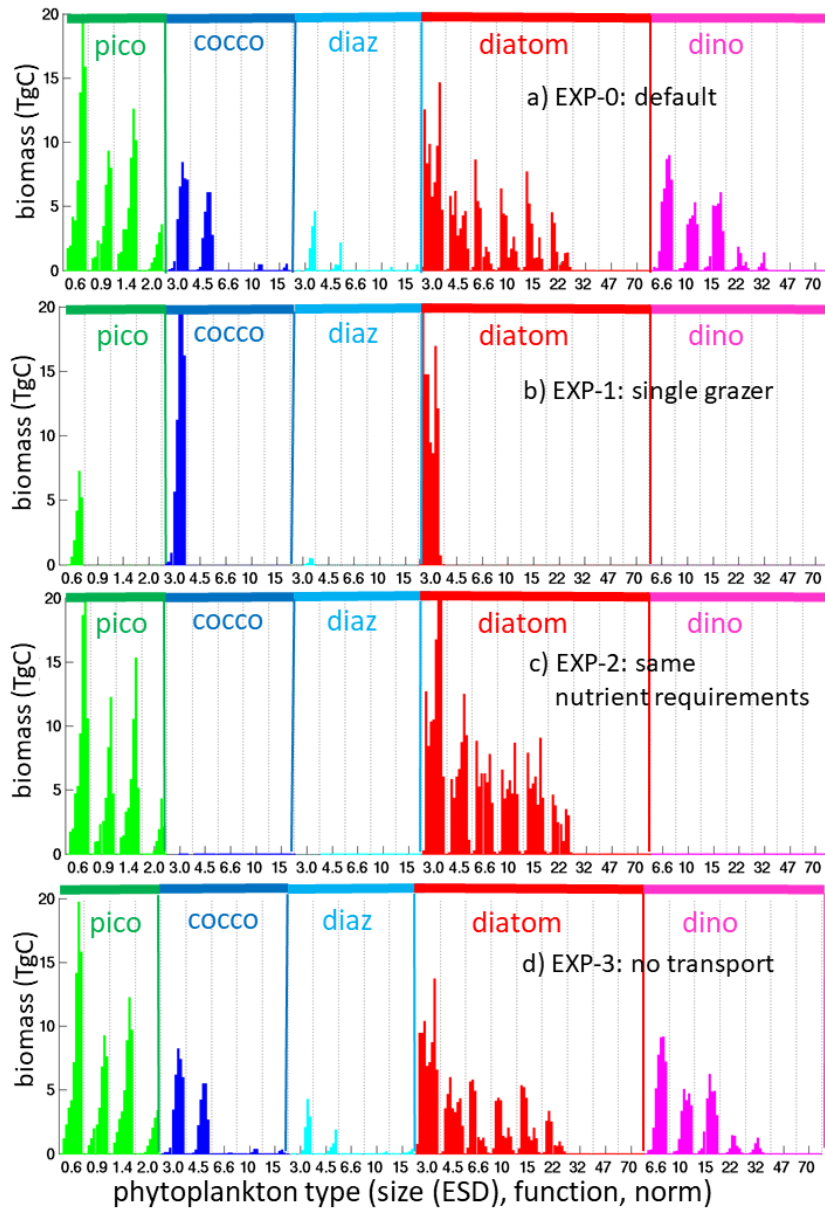
Figure 10: Sensitivity Experiments, phytoplankton global biomass. Global integrated biomass (TgC) for (a) default experiment (identical to Fig 6a); (b) EXP-1 (experiment with single generalist grazer); (c) EXP-2 (experiment where all phytoplankton have same nutrient requirements); (d) EXP-3 (experiment where plankton are not transported). Types are arranged by functional group as indicated by the colour and labels at the top of the graph, by size classes (equivalent spherical diameter, ESD) as labelled below the graph, and thermal norms from cold adapted to warm adapted from left to right in between vertical dotted lines.

1110
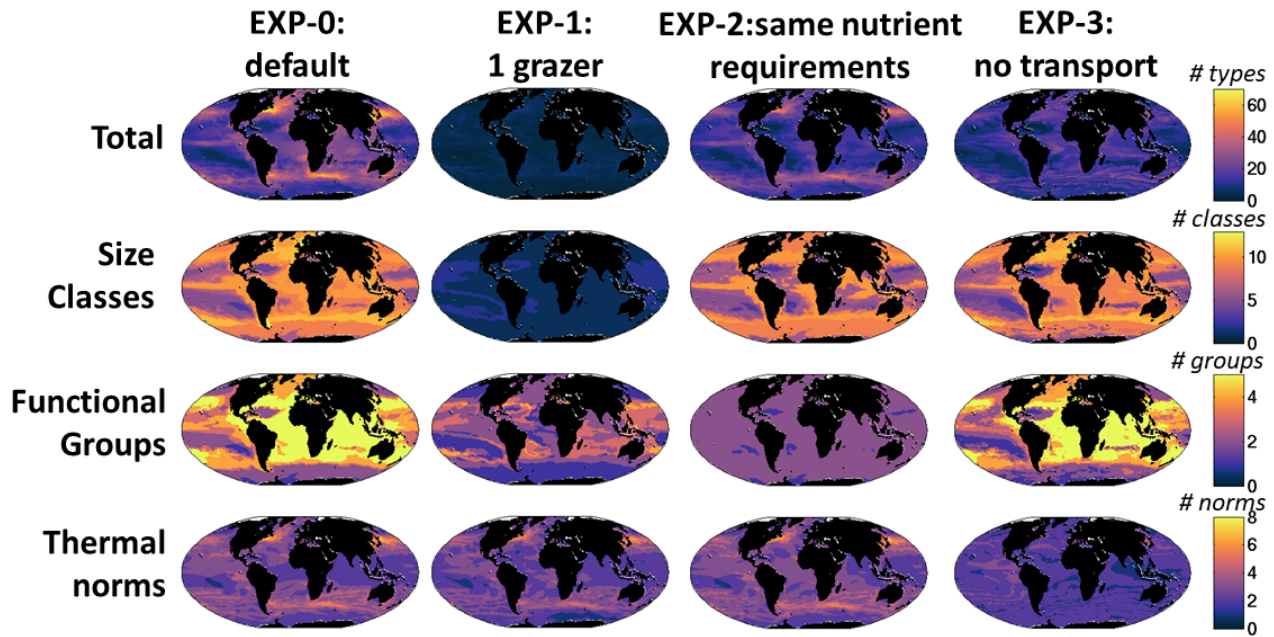
Figure 11: Sensitivity simulations, model annual mean richness. EXP-1 has no size-dependent loss rates (i.e. only one grazer); EXP-2 has no nutrient requirement differences between functional groups; EXP-3 has no transport of the plankton (all nutrients and non-living organic pools are transported). Top row: total richness; Second row: size class richness determined by number of co-existing size classes; Third row: functional richness determined by number of co-existing biogeochemical functional groups; Bottom row: thermal richness determined by number of co-existing temperature norms. The left most column are the same output as shown in Fig 8a,b,c,d for the original ("default") experiment, but with absolute values (i.e. not normalized).
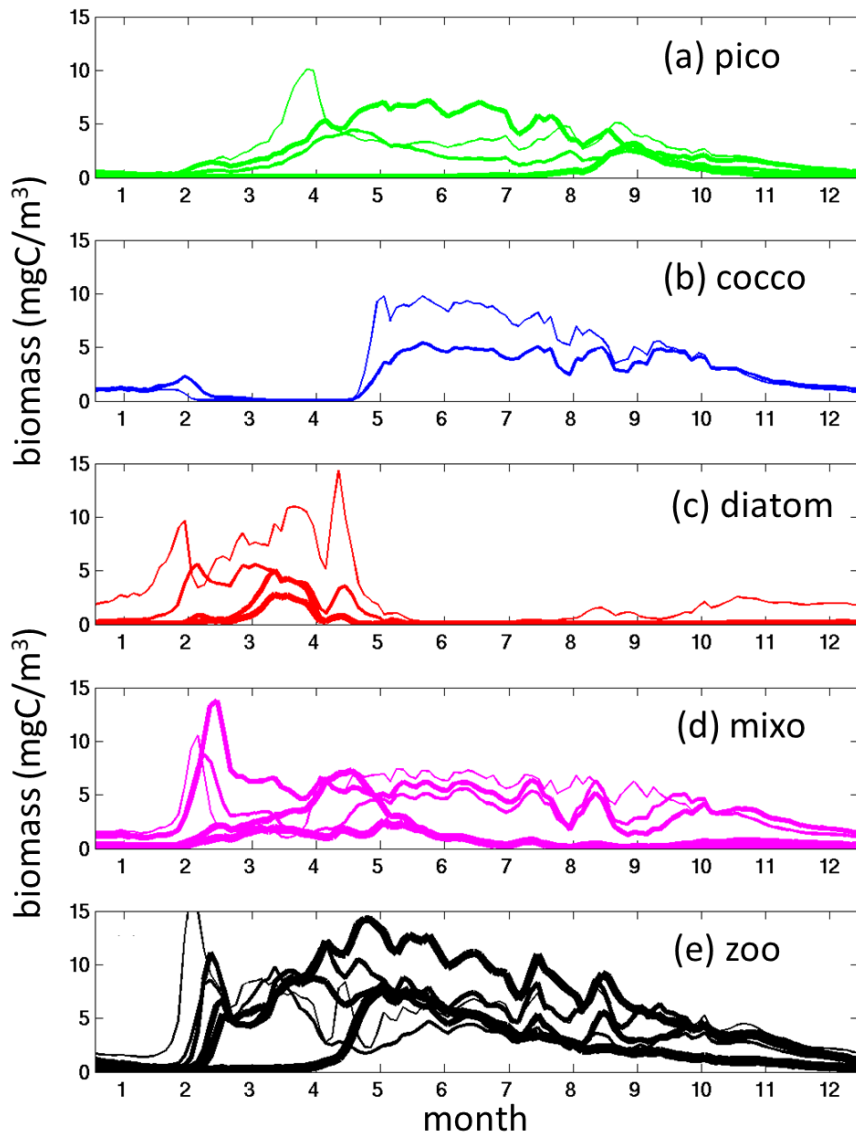
Figure 12: Default model timeseries in the North Atlantic (20ºW,45ºN). Carbon biomass (mg/m^3) of (a) pico-phytoplankton functional group binned by size class; (b) coccolithophores binned by size class; (c) diatoms binned by size class; (d) mixotrophic dinoflagellates binned by size class; (e) zooplankton by size class. Diazotrophs do not survive at this location. Thickness of lines are based from the smallest to the largest size in each functional group (i.e. thinnest line is for 0.6μm for picophytoplankton, 3μm for diatoms etc), except for zooplankton where the thickness of line is linked to the preferential diatom prey size (i.e. 30μm ESD zooplankton for the thinnest line), to show the zooplankton-diatom interactions.
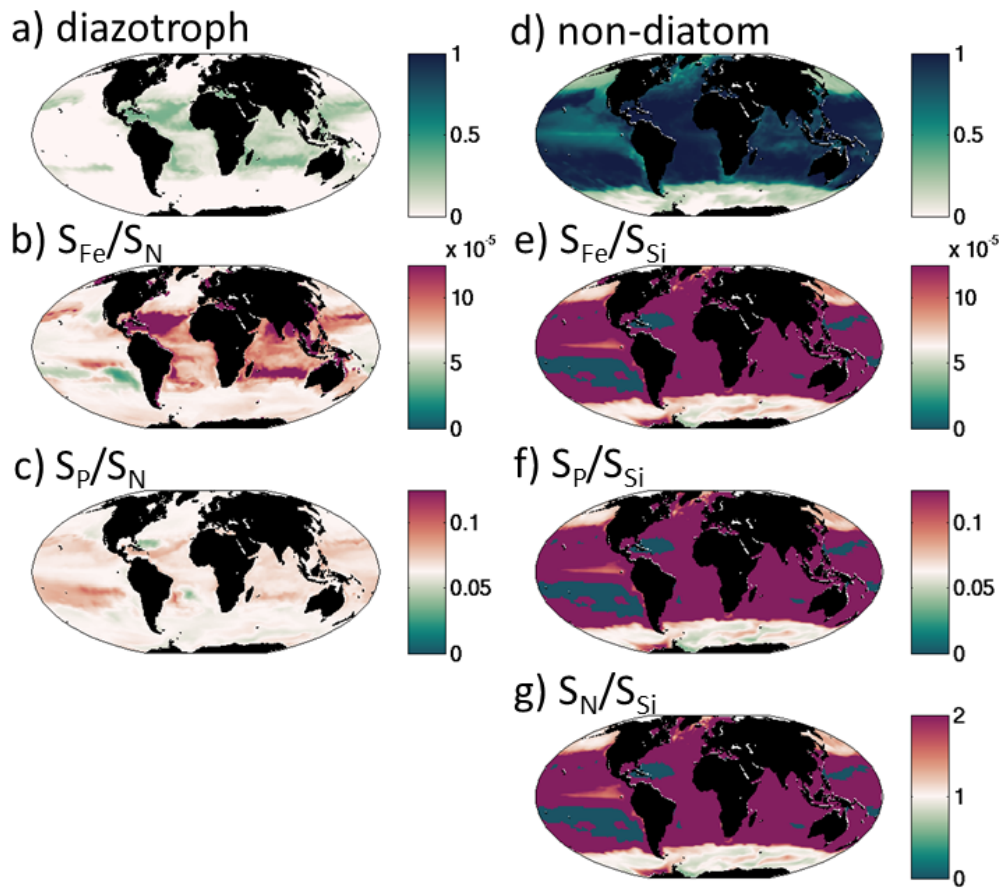
Figure 13: Co-existence of functional types defined by imbalance of different nutrient supply rates. Left column depicts controls on diazotroph distribution: (a) fraction of total biomass made up of diazotrophs; (b) ratio of iron to DIN supply rates (see Fig 9); (c) ratio of phosphate to DIN supply rate. Colour scale is chosen such that purple indicates supply rate ratios in excess of the non-diazotroph Fe:N and P:N requirements. Right panel for co-existence of diatoms and non-diatoms: (d) fraction of biomass made up of non-diatoms; (e) ratio of iron to silicic acid supply rates; (f) ratio of phosphate to silicic acid supply rate, (g) ratio of DIN to silicic acid supply rates. Colour scale is chosen such that purple indicates supply rate ratios in excess of the diatom Fe:Si, P:Si, and N:Si requirements.
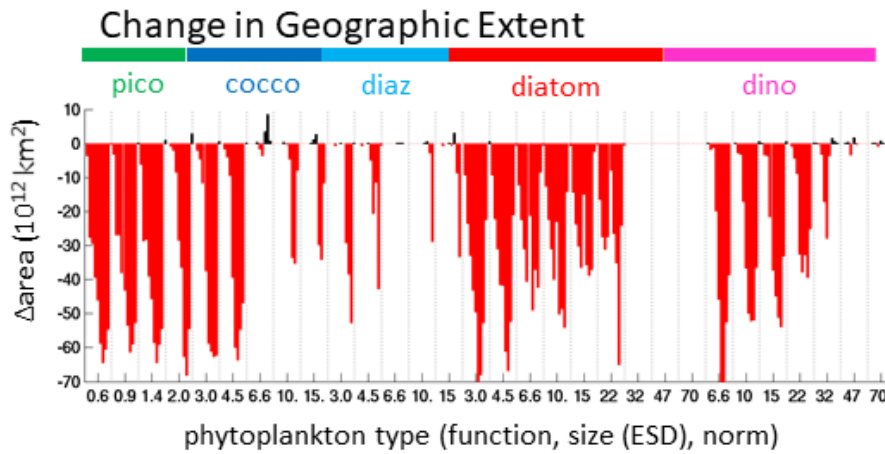
Figure 14: EXP-3 Difference in phytoplankton range geographic extent. Change in areal extent of all phytoplankton types (10^{12} km^2) between EXP-0 and EXP-3 (no horizontal transport of plankton). Negative (red) indicates a decrease in the

1140   geographic domain of the phytoplankton type. Types are arranged by functional group as indicated by the coloured labels at the top of the graph, by size classes (equivalent spherical diameter, ESD) as labelled below the graph, and thermal norms from cold adapted to warm adapted from left to right in between each vertical dotted line. Differences are relative to those shown in Fig 6b.

1145
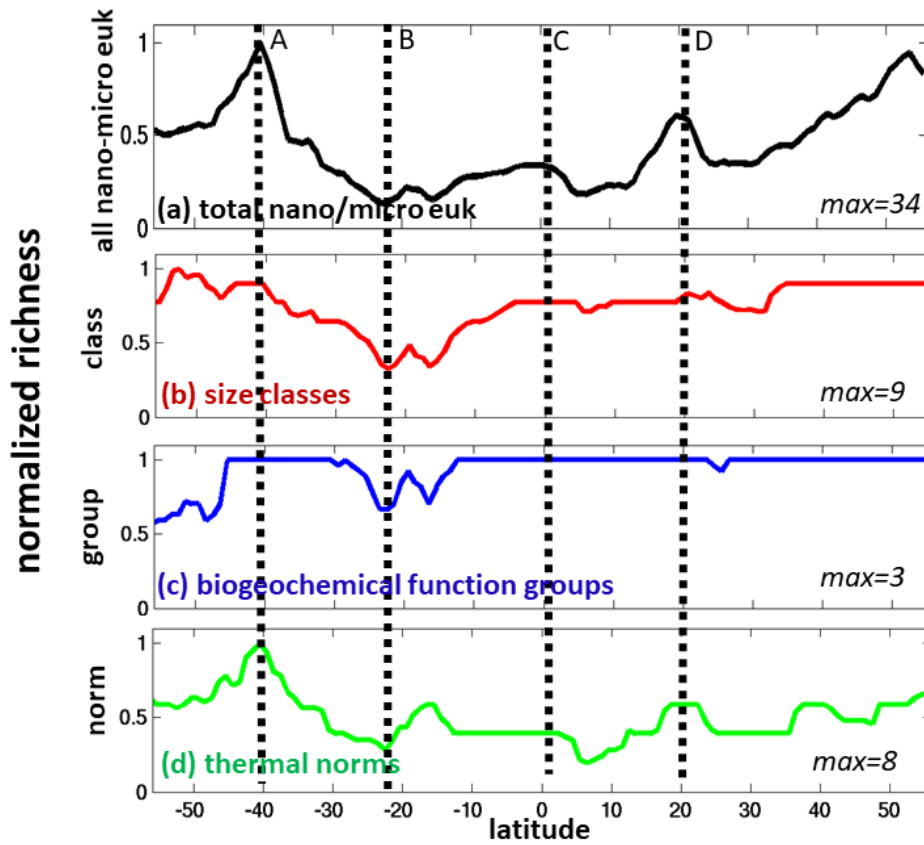
Figure 15: Modelled nano-and micro eukaryote normalized richness along Atlantic transect. Annual mean richness normalized to the maximum in a transect similar to AMT for (a) all diatoms, coccolithophores and dinoflagellates, this panel is the same as Fig 1b; (b) size classes; (c) biogeochemical functional groups; (d) thermal norms. Normalization factor is given on bottom right of each panel. Note that pico-phytoplankton and diazotrophs are not included in this analysis as they were not part of the observations. Dashed lines and text (A,B,C,D) are used to locate regions discussed in the text.

1150

1155